PREDICTION OF HIGH-SPEED SHAFT NATURAL FREQUENCIES EMPLOYING HARMONIC EXCITATION

by

Katherine Jeanne Lehmann

Thesis submitted to the Faculty of the
Virginia Polytechnic Institute and State University
in partial fulfillment of the requirements for the degree of

MASTER OF SCIENCE

in

Mechanical Engineering

W. F. O'Brien, Chairman

C. E. Knight

H. H. Mabie

December, 1983

Blacksburg, Virginia

PREDICTION OF HIGH-SPEED NATURAL FREQUENCIES EMPLOYING HARMONIC EXCITATION

by

Katherine Jeanne Lehmann

ABSTRACT

A shaft and bearing system was developed with natural frequencies in the range of 8,000 to 60,000 rpm for the purpose of determining the practicality of low-speed harmonic excitation of high-speed natural frequencies. The analytical development and analysis utilized SPAR, a finite element program, and a bearing stiffness program to determine frequencies for the first through fourth harmonics of natural frequencies under 60,000 rpm.

A misaligned flexible disc coupling was used to input a forcing function with a frequency of N times the running speed and thereby excite the natural frequencies in the Nth harmonic at the running speed.

Most of the analytical results had corresponding experimental results; however, many increased vibration levels did not correlate with analytical results. Four frequency response plots are presented. A comparison of these plots and analytical results are presented in the form of a Campbell diagram. Although the experimental results are not supportive enough to be conclusive, they do indicate that low-speed harmonic excitation may be a method of predicting high-speed natural frequencies. Major difficulties were encountered in the experimental program which are described, and some alternative investigations are proposed.

AKNOWLEDGEMENTS

I would like to express my gratitude to the Mechanical Engineering Machine and Instrumentation Shop personnel, especially Johnny Cox and Jerry Lucas, whose help was invaluable.

I also wish to thank my committee members, especially Dr. O'Brien, and Dr. Larry Mitchell for their support during this project.

I am grateful for the financial support from Industrial Drives Division of the Kollmorgen Corporation and the encouragement and assistance from Mr. Ed Phipps.

I am also appreciative of the patience and flexibility that Mr. Ernest Screen has had concerning my future employment.

Special thanks are extended to my parents, Dr. William L. Lehmann and Mrs. Barbara T. Lehmann, and to Jim Williams for their love, patience, and support.

Finally, I wish to express my gratitude to my fellow graduate students and friends, especially Tammy Finn, Marty Harsh, John Menna, Pat and Bart Nnaji, Lisa O'Hara, and Wayne Burstein, for their support and comradeship.

TABLE OF CONTENTS

LIST OF FIGURES

LIST OF TABLES

1. INTRODUCTION

Natural frequencies of rotating equipment can cause costly damage if they exist in the operating range of the equipment. Problems such as fatigue, bearing seizures, and rubbing are much more likely to occur at a natural frequency than at other speeds. Equipment is designed and modified to avoid and move natural frequencies. Often a vibration problem arises in existing equipment and natural frequencies must be determined in order to solve the problem. Various methods available for determining natural frequencies are 1) impulse hammer testing, 2) swept sine testing, 3) Sine Order Analysis (SORAN)*, and 4) analytical modelling, such as transfer matrix or finite element methods.

Impulse hammer testing utilizes a hammer with an accelerometer mounted on the back of the hammer head and an accelerometer mounted on the structure of interest. The hammer is used to send an impulse through the structure. The accelerometer on the hammer head is used to monitor the impulse sent, and the accelerometer on the structure is used to monitor the impulse after it has passed through the structure. The received signal may or may not have enough amplitude to be useful.

Swept sine testing employs a sinusoidal force which is swept through the frequency range of interest and input to the test structure [1]. The force is commonly generated by a shaker table. An accelerometer is used to pick up the signal transmitted through the structure.

---

* SORAN is a registered trademark of the Zonic Corporation.

[1] References are denoted by numbers in brackets and are listed after the recommendations section.

Both of the above methods require rotating equipment to be out of operation while testing. SORAN, however, requires the equipment to be run through the speed range of interest while taking data. A vibration sensor such as an accelerometer or a proximeter probe is used to monitor vibration. The data are acquired, processed, and displayed by the ZONIC 6080 FFT. For each of the above methods, a frequency plot is generated and natural frequencies can be read from the plot if the received signal is large enough.

For determining natural frequencies of rotating equipment, data taken while equipment is operating should be more accurate. This is because bearing stiffnesses change as running speed changes due mainly to centrifugal forces, and natural frequencies are functions of system stiffness. Figure 1.1 is an example of bearing stiffness as a function of speed [2]. Because natural frequencies are functions of system stiffness they will also change as a function of running speed, following the general trend of the appropriate bearing stiffness curve.

Analytical models are also useful tools for determining system natural frequencies and can easily account for changes in bearing stiffness. Many computer models using transfer matrix and finite element methods are available. The following is a general matrix equation.

$$[M][\ddot{X}] + [K][X] = [0]$$

The mass matrix, [M], is the coefficient of the acceleration matrix, $[\ddot{X}]$. The stiffness matrix, [K], is the coefficent of the displacement matrix, [X]. Most available software do not handle

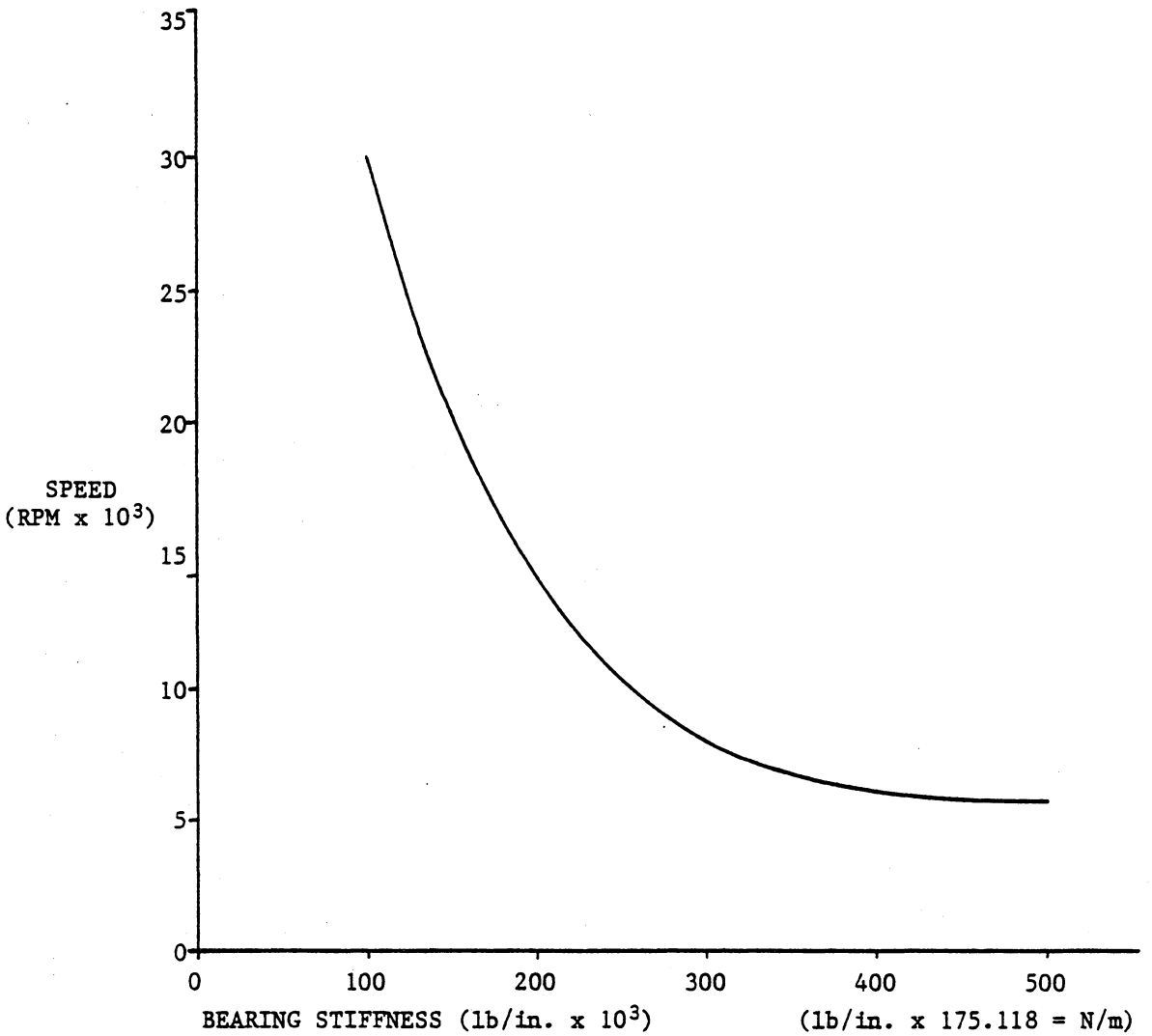

Figure 1.1 A Typical Bearing Stiffness Curve
(Taken from Reference 2)

variable coefficients. Therefore, different bearing stiffnesses are entered for particular speeds of concern so that the coefficent of [X] is constant.

Bearing stiffnesses are not generally available from bearing manufacturers; however, computer models can be used to determine stiffnesses. Van Winkle [3] developed a computer program modelling bearings based on T. Harris' equations. The program handles axial and radial loading, accounts for contact angle and centrifugal force, and gives deflection in the output. The stiffness must then be hand calculated using deflection and applied loads. This program has convergence problems for predominantly radial loads [4], thereby limiting its usefulness for such applications. A bearing program developed by Shaker Research Corporation for the U.S. Air Force* [5] handles axial and radial loads, combined or separate. It accounts for contact angle, material characteristics, and centrifugal force. The output gives bearing stiffness in a complete 5 x 5 matrix, reactions of bearings on shafts, and bearing displacements.

Another possibility for determining natural frequencies is to combine computer modelling and experimental testing. A shaft in operation excited at n times per revolution can experience vibration modes that are at n times the running speed, or the n^{th} harmonic. This has long been evident in turbomachinery operation. H. Stargardter refers to this as per-revolution excitation in reference to turbofan aircraft, noting that when a "natural resonant frequency of a fan stage coincides

---

* This is referred to as the "Air Force" bearing program throughout this paper.

with the frequency of the source, severe vibration usually results." [6] A common source of per-revolution excitation is a stator preceeding a rotor. Here the rotor blades are excited by wakes from the stator. Turbine blades are designed to avoid natural frequency modes. Campbell diagrams, such as Figure 1.2, show natural frequency modes and n-per-revolution forces as functions of running speed. For a particular operating speed, the equipment should be designed so that the natural frequencies are between the harmonic frequencies [7] [8].

Another area where n-per-revolution forces are encountered is that of flexible couplings. Fleeting and Coats note that "Flexible (gear) couplings such as those fitted to turbines . . . give rise to torsional fluctuations at frequencies equal to tooth frequency when simple misalignment of shafts occur" [9]. Wright [10] notes that flexible couplings generate cyclic and steady forces and moments within themselves when misaligned, and that when the forced vibration loads have a frequency coinciding with the natural frequency of the rotating-shaft-system, vibration resonance may be excited. He also gives equations for frequencies of forces and moments generated by several types of couplings and notes that a frequency of twice the running speed (2N) may be associated with all couplings due to imperfections in the manufacturing process. D. L. Dewell and L. D. Mitchell [11] [12] discuss detection of misaligned couplings using a Real Time Analyzer and give equations of forces- and moments- per-revolution present in misaligned couplings (Hooke's, Crowned Tooth Gear, and Metallic Disc Couplings). They also performed tests on misaligned metallic disc couplings showing 2-per-revolution and 4-per-revolution forces detected.

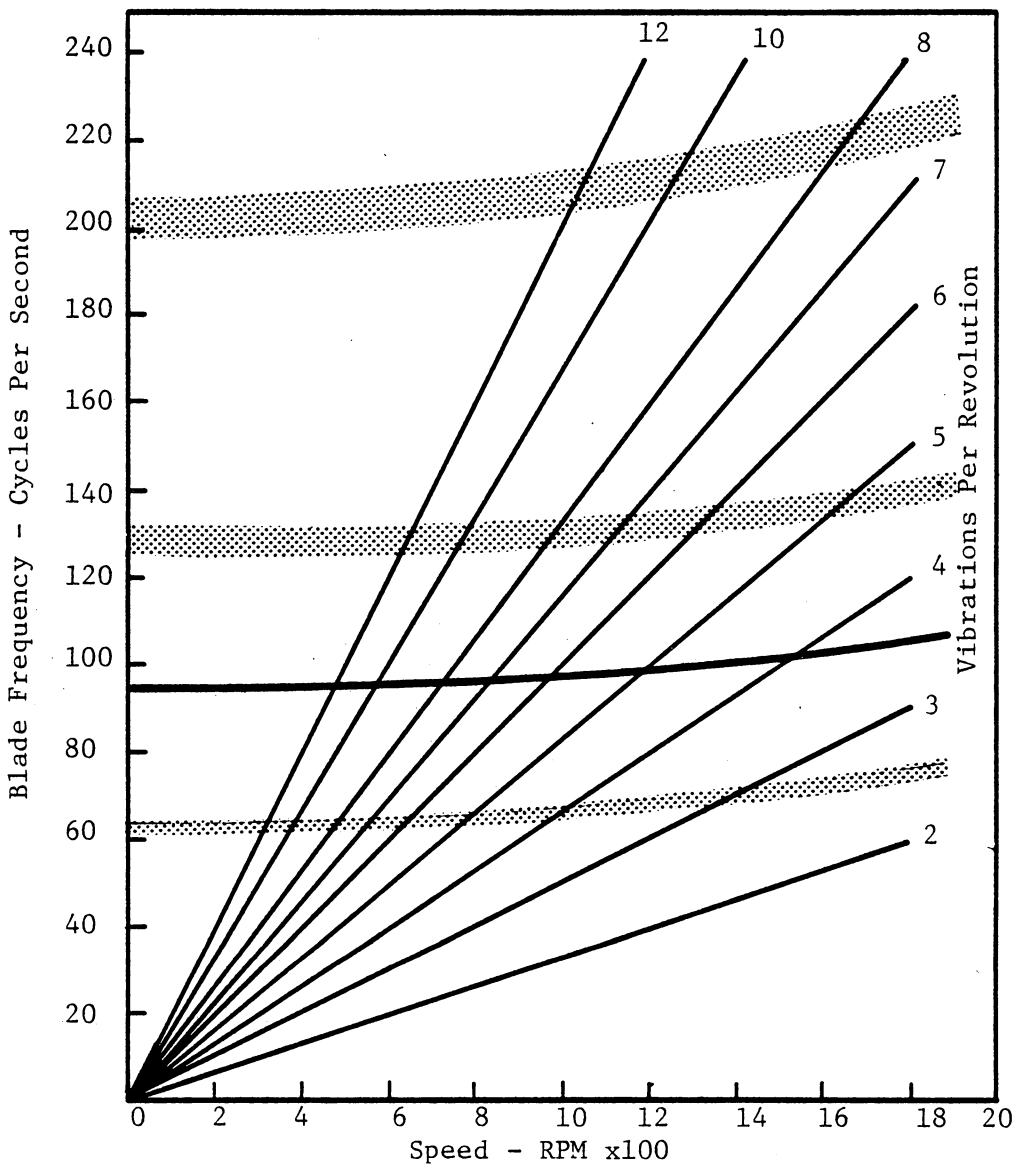

Figure 1.2 Example of a Campbell Diagram
(Taken from Reference 8)

The purpose of the present research is to determine if a flexible disc-coupling exciting n^{th}-order-harmonics can successfully be used to predict critical frequencies. In particular, there is interest in determining high-speed critical frequencies with low-speed excitation of higher-order harmonics employing a misaligned coupling. A computer analysis using SPAR [12] (a system of programs for mechanical design problems) and the bearing stiffness program developed by Shaker Research Corporation [5] are used to design a shaft for testing and to predict its critical and harmonic frequencies. Tests are conducted with SORAN to confirm critical frequencies and their harmonics. Test results are presented in tabular and graphical forms and are compared to the analytical predictions.

2. ANALYTICAL MODEL

The tools employed for design and analysis of the test shaft-and-bearing system are SPAR and the Air Force bearing stiffness program. SPAR is a system of programs used for linear finite element analysis of mechanical systems. Finite Element Analysis (FEA) utilizes a model composed of elements of finite sizes. Elements are joined at nodes which each have n-degrees of freedom. System matrices, describing the entire network of elements and nodes, are formed to be used during analysis. Static and dynamic analysis can be performed. SPAR is primarily for stress, buckling, and vibration analysis. For this research SPAR is used to develop an appropriate test shaft and to determine its natural frequencies and mode shapes.

A suitable system model is developed by 1) considering constraints imposed by equipment, 2) constructing preliminary models to determine an appropriate shaft size, and 3) constructing a more detailed model of a particular test shaft. The driving unit imposes major constraints on the test system. The drive unit is an air-driven high-speed drive adapted from an automobile turbocharger. This drive system is described in Appendix A. It has a natural frequency in the range of 30,000 to 35,000 rpm and increasingly high vibration levels above 70,000 rpm. It is also difficult to increase running speed slowly enough to gather data in the desired fashion for speeds under 8,000 rpm for this drive system. Therefore, a shaft for which critical speeds are being monitored should have critical speeds in the ranges of 8,000 rpm to 30,000 rpm and 35,000 to 70,000 rpm, preferably under 60,000 rpm.

Additional constraints are imposed by the desire to use an available set of side-plates and end-plates for the test shaft. These plates are shown in Fig. 3.1. The length of the side plates sets the length of the shaft between the bearings. Also, the bearing type previously used with these end-plates, the Barden 106H, is used for this research to reduce the amount of modification needed.

Several parameters may be varied in order to design critical speeds in the desired ranges. These are 1) bearing stiffness, 2) length, 3) diameter, and 4) material. The first two, bearing stiffness and shaft length, are set for this research because of side-plate dimensions and bearing selection. Shaft diameter and material are remaining design variables to place the natural frequencies into the desired speed range.

To determine an approximate range and the manner in which the natural frequencies change, the following shafts were considered: 1) a 1" diameter steel shaft, 2) a 2" diameter steel shaft, and 3) a 2" diameter aluminum shaft (see Fig. 2.1). SPAR is used to construct and analyze the models.

The SPAR model elements employed general beam elements (element type E21) for the shaft and direct stiffness elements (element type E22) for the bearings. Both element types utilize five degrees of freedom. These are displacements in the X, Y, and Z directions, and rotations θX and θY where Z is the axis of rotation. X and Y are radial directions at 90^{o} to each other. Z is the axial direction at 90^{o} to X and Y. θX and θY are the angles of twist about X and Y, respectively. The shaft elements used in the models account for general beam characteristics such as length, mass, bending, and torsion; however, for

1" Diameter Steel Shaft

2" Diameter Steel Shaft

2" Diameter Aluminum Shaft

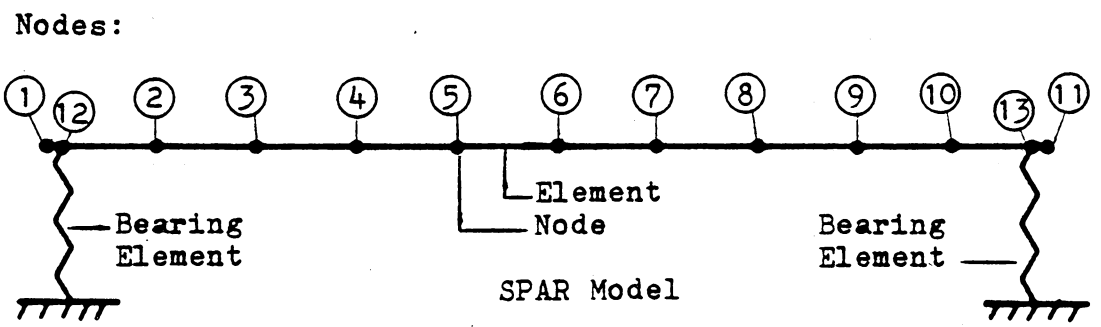

Figure 2.1 Preliminary Shaft Models

these particular models, the elements were not set up to include transverse shear deflection, rotatory inertia, and gyroscopic effects. Rotatory inertia and gyroscopic effects increase as speed increases and may affect model response. The matrix for this element type is generated by SPAR subroutines. Bearing elements are grounded at one end (all degrees of freedom fixed) and connected to the shaft at the other end (5 degrees of freedom). Grounding assumes that the support stiffness is considered rigid. Direct and coupled stiffnesses in the bearing are included. The matrix corresponding to this element type is entered directly to the input of the TAB subroutine of SPAR.

The stiffness matrix corresponding to the bearing elements is generated using the Air Force bearing stiffness program. A stiffness matrix is generated for each running speed of interest since stiffness changes as speed changes. Running speed, bearing loads, and bearing characteristics are entered in the program input (see Table 2.1). Axial loads for the test bearings are due to a thrust preload. Radial loads entered are due to the shaft weight. Both remain constant for a particular shaft model. The program output is a five by five bearing stiffness matrix accounting for direct and coupled stiffnesses for the X, Y, Z, θX, and θY directions. This matrix is entered in the input to the TAB subroutine of SPAR.

Analysis of each of the three preliminary shafts were completed. The shaft weights were calculated to determine radial bearing load (see Table 2.2). Stiffnesses for each model were computed for 10,000 rpm and 60,000 rpm, the limits of the speed range of interest. Then SPAR subroutines were run in the following order to compile system matrices

TABLE 2.1 Barden 106H Data for Bearing Program

Parameter	Value
Number of Balls	14
Ball Diameter	0.28125 inches
Pitch Diameter	1.72 inches
Contact Angle	15.0^{o}
Outer Race Curvature	0.52
Inner Race Curvature	0.52
Poisson's Ratio	0.25
Modulus of Elasticity	29×10^{6} psi
Ball Density	0.283 lb/in^{3}
Running Speed, RPM	Varies
Radial Load	Varies
Axial Load	35 lb

TABLE 2.2 Preliminary Shaft Weights and Bearing Loads

Material	Diameter	Weight (lb)	Radial Bearing Load (lb)
Steel	1"	3	1.5
Steel	2"	12	6.
Aluminum	2"	4	2.

and perform eigenvalue searches. A brief description of each subroutine is presented in Appendix B, followed by the necessary input files.

TAB

ELD

TOPO

EE

EKS

K

INV

M (RESET G = 386.)

EIG

VPRT.

Eigenvalues and corresponding mode shapes are output into file VPRT FT31 D. Mode shapes for a particular eigenvalue are represented by relative displacements of nodes in the various directions. The predominant mode shape is that of the direction(s) of the highest relative displacements.

Each of the three preliminary models has eigenvalues in the range of 10,000 rpm to 60,000 rpm (see Table 2.3). This suggests that the diameter range and material types of the preliminary models are appropriate for a test shaft.

A 1.5" diameter steel shaft was available for testing. Because its size and material were appropriate, it was modelled in greater detail. Figure 2.2 shows the shaft and its corresponding SPAR model. The weight of the 1.5" diameter steel shaft is calculated to determine the radial loads imposed on the bearings. Half of its weight is used as the radial

Table 2.3 Expected Critical Speeds for Preliminary Designs

n^{th} Eigenvalue	Shaft	Critical Speed (rpm)	
		Using Bearing Stiffness @ 10,000 rpm	Using Bearing Stiffness @ 60,000 rpm
1^{st}	1" D-Steel	25,944	21,515
	2" D-Steel	28,527	26,475
	2" D-Alum.	44,864	33,120
2^{nd}	1" D-Steel	28,313	25,946
	2" D-Steel	39,682	27,491
	2" D-Alum.	47,869	41,692
3^{rd}	1" D-Steel	56,806	51,246
	2" D-Steel	43,971	28,832
	2" D-Alum.	51,173	43,173

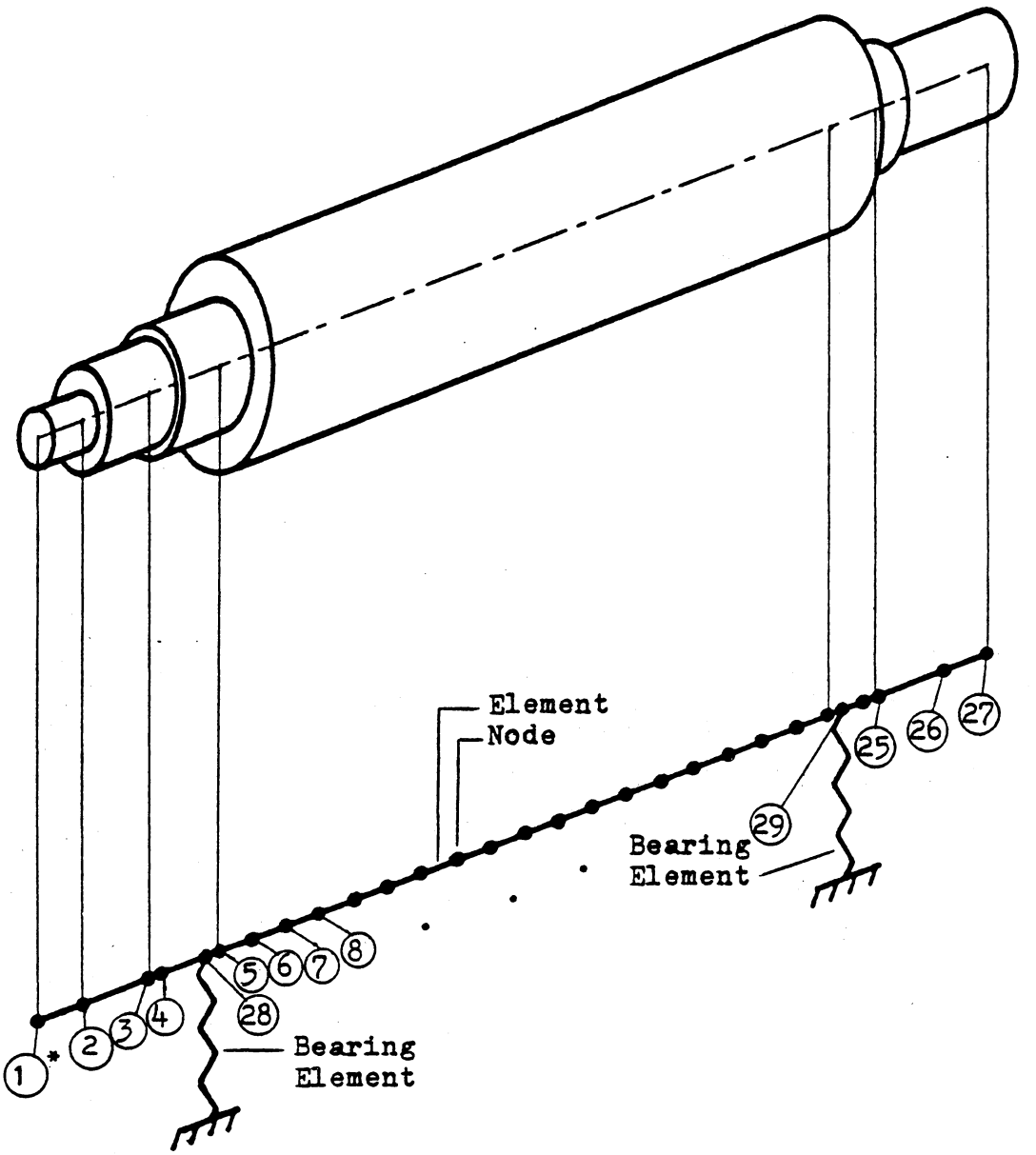

*These are node numbers

Figure 2.2 1.5" Diameter Steel Shaft Model

load for computing each bearing stiffness using the Air Force bearing program. Analyses employing bearing stiffnesses corresponding to 60,000 rpm indicate that the first five natural frequencies may be under 60,000 rpm. For a bearing stiffness corresponding 10,000 rpm, only the first three natural frequencies are under 60,000 rpm. Bearing stiffnesses were computed for running speeds of 3,000 rpm to 60,000 rpm and are plotted in Fig. 2.3. The stiffness drops rapidly as the running speed increases up to approximately 30,000 rpm, from which it increases slowly as running speed increases. A rough estimate for the natural frequency of a spring and mass system is $\sqrt{K/m}$, where K is the equivalent-system stiffness and m is the equivalent-system mass. Because natural frequency is roughly proportional to the square root of the stiffness, it may be expected that eigenvalues (as a function of speed) may follow the same general pattern as bearing stiffness as a function of speed.

Eigenvalue searches were completed using bearing stiffnesses corresponding to 10,000 rpm and 60,000 rpm. Next, stiffnesses at running speeds corresponding to the eigenvalue frequencies determined from the 60,000 rpm eigenvalue search were used for model input for convergence on predicted eigenvalues 1, 2, 3, 4, and 5. Interpolation was used to more accurately approximate actual eigenvalues. Stiffnesses corresponding to these values were entered for further eigenvalue searches. This convergence process was continued until eigenvalue frequencies and running speeds corresponding to bearing stiffnesses entered were within 50 rpm (0.83 Hz) of each other. The first five eigenvalues found using SPAR are presented in a Campbell diagram in Fig. 2.4. Note that if the bearing stiffness were not a function of running

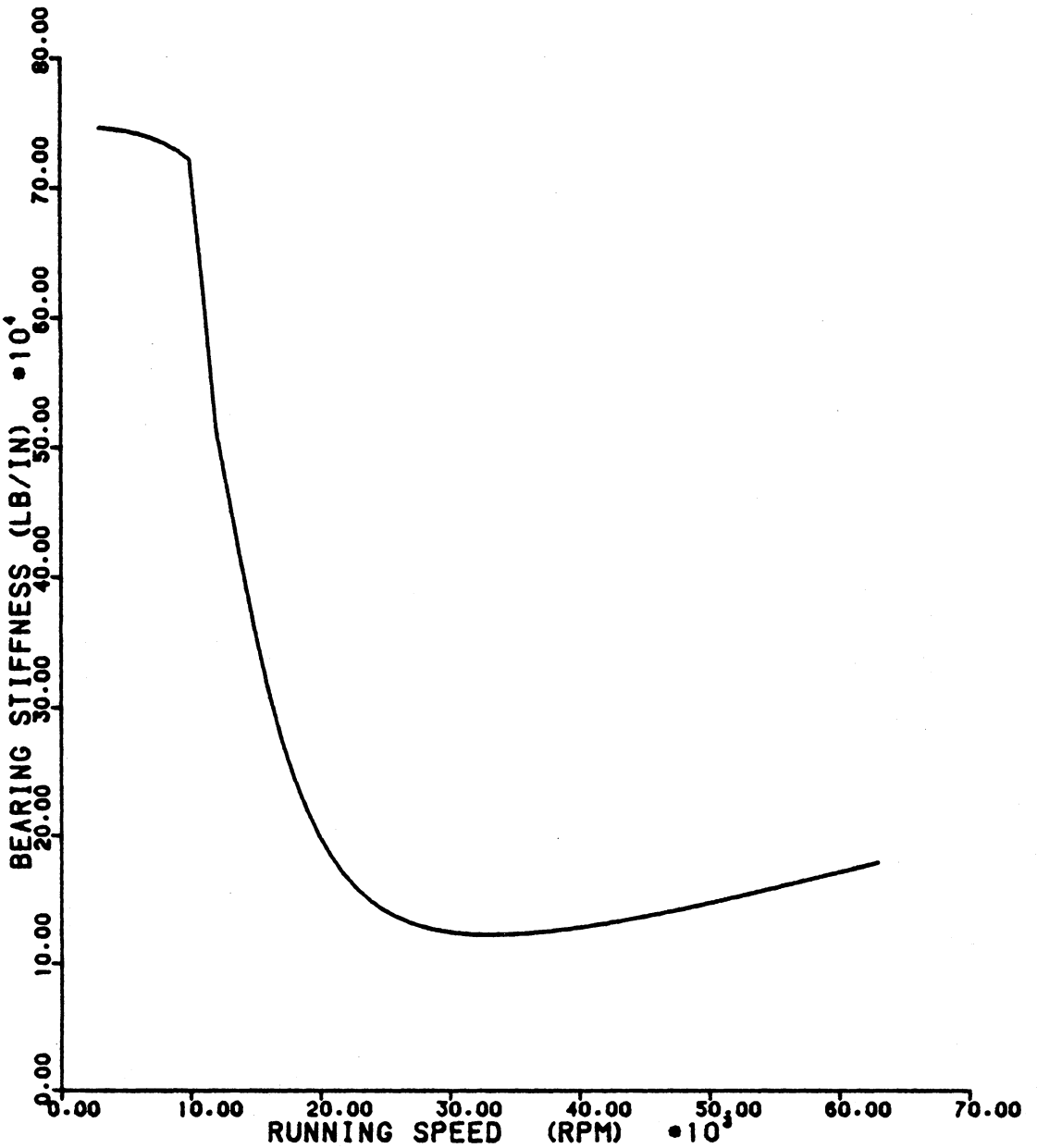

Figure 2.3 Bearing Stiffness Curve Over Operating Range

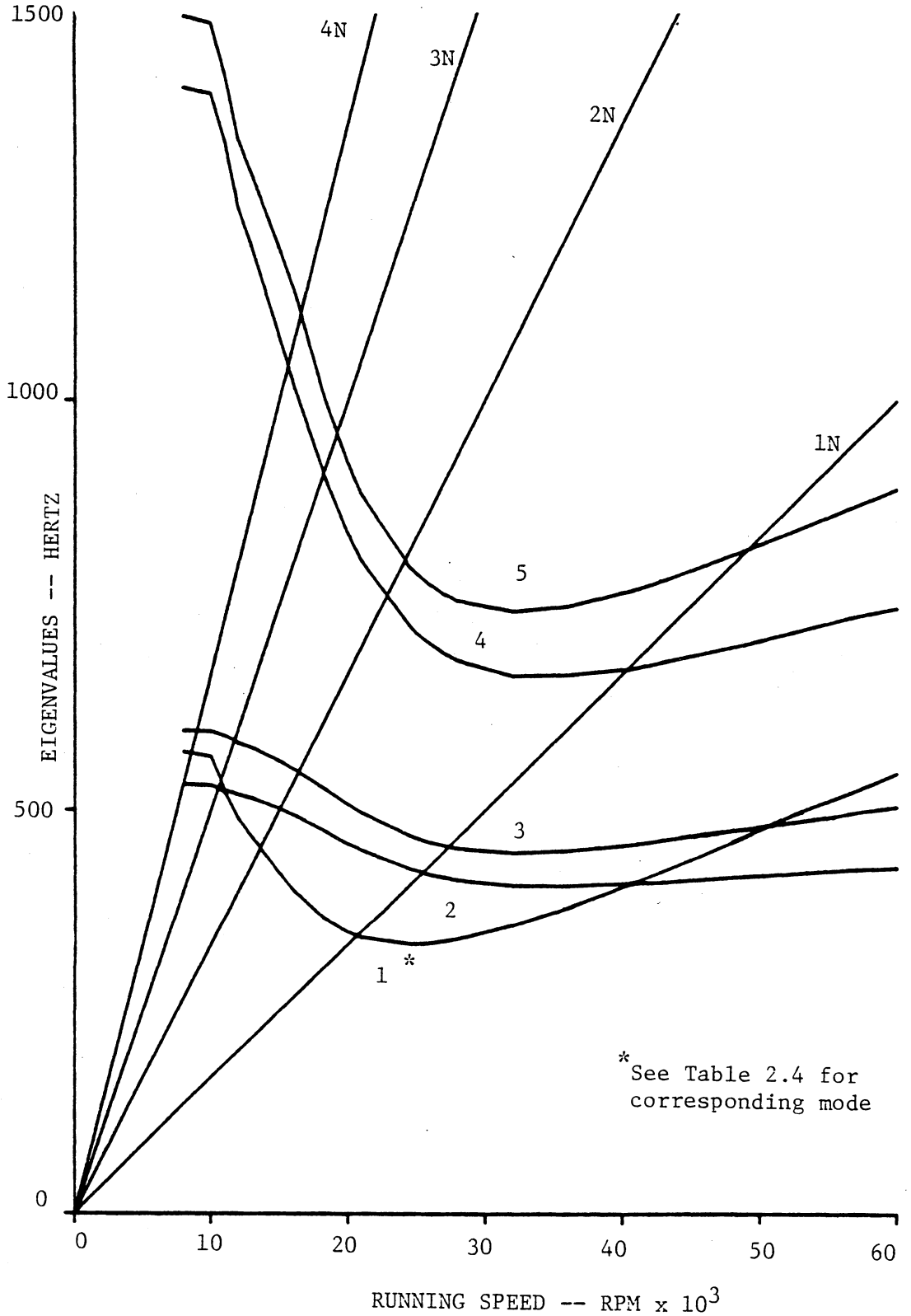

Figure 2.4 Campbell Diagram for 1.5-Inch Diameter Steel Shaft

speed, the eigenvalues would be constants with respect to running speed. The first five expected resonant frequencies of this shaft are 20650, 25400, 27350, 40450, and 49130 rpm. These are frequencies that are excited by 1/rev excitation. Table 2.4 shows the mode shape of each natural frequency. Each natural frequency has relative shaft displacements in either the X- or the Y-direction.

N/rev Input

Two methods for exciting the shaft at multiples of the running speed were considered. One was to have interchangeable sinusoidal cams attached to one end of the shaft and a follower applying a force proportional to displacement to the cam, as shown in Fig. 2.5. Two-, three-, and four-lobed cams will cause sinusoidal force inputs to the shaft at two, three, and four times the running speed, respectively. The other method was to couple the test shaft to the drive shaft, slightly misaligned, with a flexible disc coupling. According to Wright [10] and Dewell [11,12] the basic vibration frequency due to a misaligned disc coupling is

$$F = Nn \text{ for an even } n$$

and $$F = 2Nn \text{ for an odd } n$$

where F = vibration frequency

N = shaft speed

n = number of disc fastening bolts,

or 4N for a disc coupling with four bolts. Forces and moments at 4-per-revolution are produced as the bolts pass through high stress positions. Point A in Fig. 2.6 shows the position for a maximum moment

Table 2.4 1.5" Diameter Test-Shaft Mode Shapes

Mode Shape	
	w_1 = 344 Hz (20650 rpm)
1 2nd Rigid Mode X-direction	
	w_2 = 423 Hz (25400 rpm)
2 1st Bending Mode Y-direction	
	w_3 = 456 Hz (27350 rpm)
3 1st Bending Mode X-direction	
	w_4 = 674 Hz (40450 rpm)
4 2nd Bending Mode X-direction	
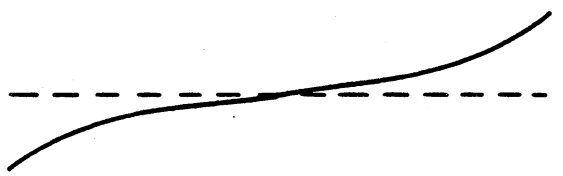	w_5 = 819 Hz (49130 rpm)
5 2nd Bending Mode Y-direction	

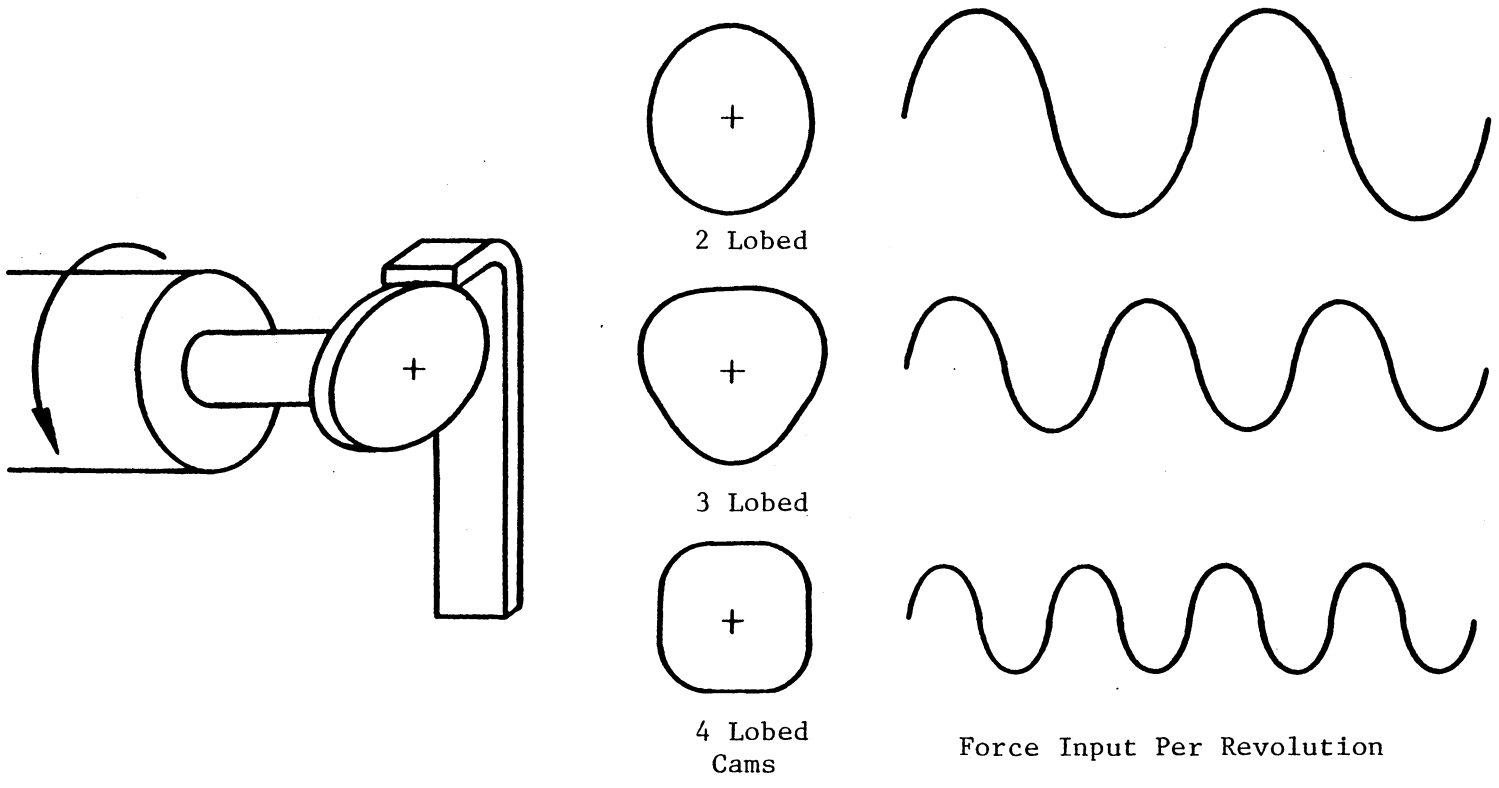

Figure 2.5 Lobed Cams and Follower

to be produced. Figure 2.7 shows the moments produced in one revolution.

The method employing cams was not selected for various reasons. A principal reason was the unknown effects of loading of the shaft and bearings in this fashion at speeds up to 40,000 rpm. Selecting or designing a follower suitable for the application with an adequate lubrication system becomes a problem. Also, high acceleration levels are anticipated and balancing for these speeds would be difficult.

The method using disc couplings presented fewer problems. Disc couplings are readily available, and need no lubrication system. The magnitude of the force inputs can be changed by changing the alignment. The following analysis is done for a Thomas flexible disc coupling.

According to Dewell, there are several expected vibration frequencies other than the basic 4N. These are 2N and harmonics of 4N $\pm$N, or 2N, 3N, 4N, 5N, 7N, 8N, 9N, etc. The 2N frequency is due to imperfections in the manufacturing process. 3N, 4N, 5N and 7N, 8N, 9N, etc. are the harmonics of 4N $\pm$ N.

As mentioned before, if the bearing stiffnesses were constant for all speeds, then each natural frequency should show up at 1/2, 1/3, and 1/4 of its speed in the 2nd, 3rd, and 4th orders of the vibration signal, respectively. But the stiffnesses change and must be modelled as such. The natural frequencies occur when the frequency of the eigenvalue is equal to the running speed. These are at the intersections of the eigenvalue curves and the one vibration-per-revolution, or 1N, line (see Fig. 2.3). The second, third, and fourth order harmonics of each

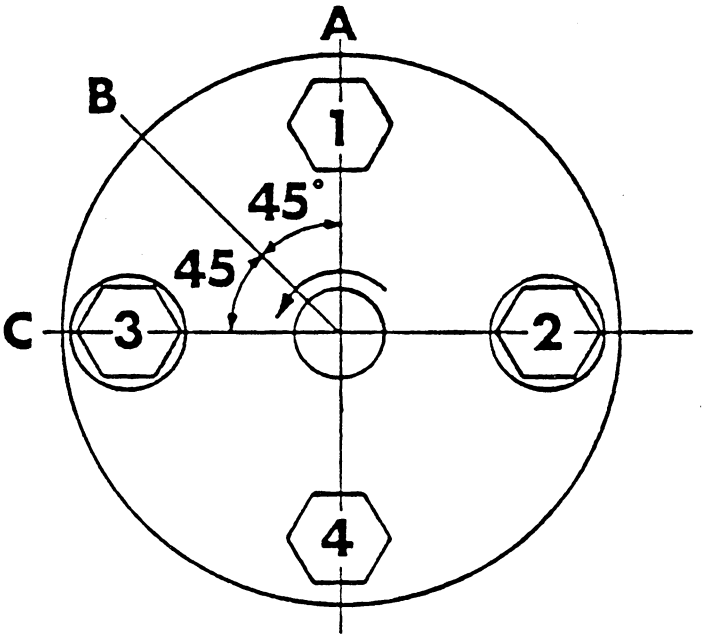

End View from Left

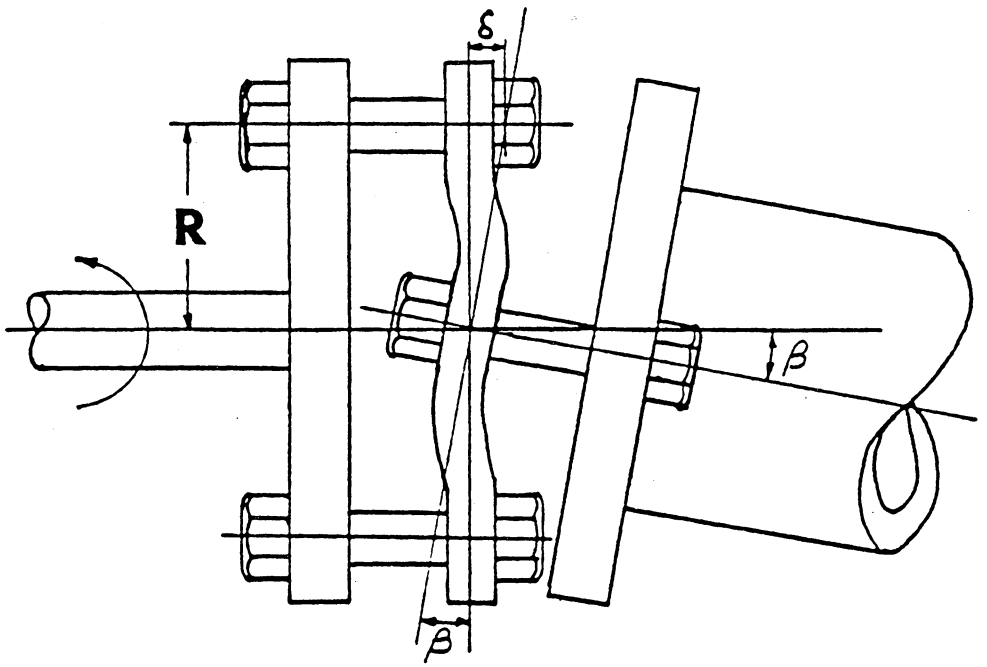

Figure 2.6 Misaligned Disc Coupling (Taken from Reference 11)

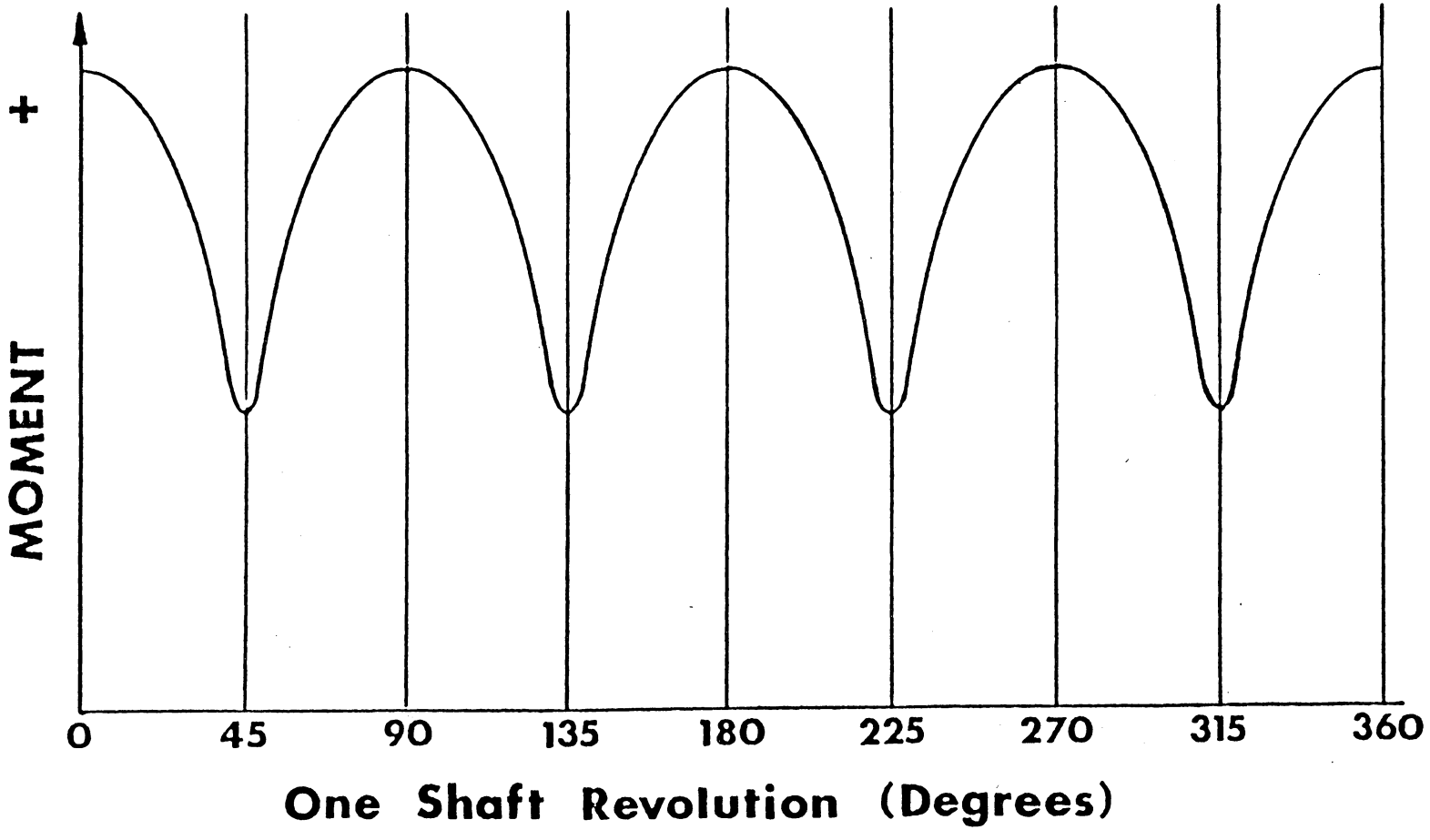

Figure 2.7 Moments Produced in One Revolution of Misaligned Disc Coupling (Taken from Reference 11)

natural frequency occur when the eigenvalue frequency is equal to two, three, and four times the running speed, respectively. Expected natural frequencies and their harmonics were determined as previously described using SPAR subroutines and are presented in Table 2.5.

Table 2.5 Frequencies and Running Speed of Expected Harmonics

Mode Shape (direction)	Harmonic # 1 F(Hz)* (N (rpm))	2 F(Hz) (N (rpm))	3 F(Hz) (N (rpm))	4 F(Hz) (N(rpm))
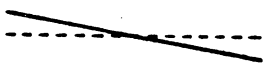 1 2nd Rigid Mode X-direction	344 (20,650)	453 (13,600)	535 (10,700)	570 (8,550)
 2 1st Bending Mode Y-direction	423 (25,400)	502 (15,045)	529 (10,575)	530 (7,950)
 3 1st Bending Mode X-direction	456 (27,350)	547 (16,400)	584 (11,685)	597 (8,960)
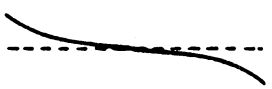 4 2nd Bending Mode X-direction	674 (40,450)	758 (22,750)	911 (18,220)	1043 (15,640)
 5 2nd Bending Mode Y-direction	819 (49,130)	805 (24,150)	960 (19,200)	1107 (16,600)

* F is frequency in Hertz. N is running speed in rpm.

3. EXPERIMENTAL SET-UP AND PROCEDURES

The experimental equipment is listed in Table 3.1. The arrangement of the mechanical equipment is shown in Fig. 3.1. The turbocharger is driven by compressed air fluctuating between 95 psig and 115 psig, and at room temperature. It is loaded by adjusting a valve on the outlet hose of the compressor. The cooling and lubricating oil (30 W motor oil) is kept between 40 and 50 psig. This pressure is necessary particularly for higher speeds, (as, for example, 30,000 rpm and above), to avoid damage to the journal bearings in the turbocharger. A shaft extension screwed onto the compressor end of the turbocharger shaft and supported by a perforated cylindrical housing serves as the drive shaft coupled to the rotor being tested. A description of this high-speed turbocharger rotor-drive is presented in Appendix A. An accelerometer is mounted on the drive-shaft housing. A Thomas 12CC coupling slides over the end of each shaft and is fixed in place by tightening the set screws. The outer radius of the coupling flange is polished and painted a flat black over 180^{o} so that the speed pick-up produces a once-per-revolution signal. The speed pick-up works on the basis of reflectivity, producing a voltage inversely proportional to the amount of light neglected. The test shaft is supported by bearings on each end and enclosed in steel side- and end-plates 3/8" thick for protection. The top side plate and one of the side-plates have provision for slide-mounts and a slot for eddy-current proximeter probes to be positioned properly next to the shaft. The bottom side plate is mounted onto a sliding base plate so that the test shaft can be slid back and forth and the coupling easily mounted. There is also extra clearance permitting

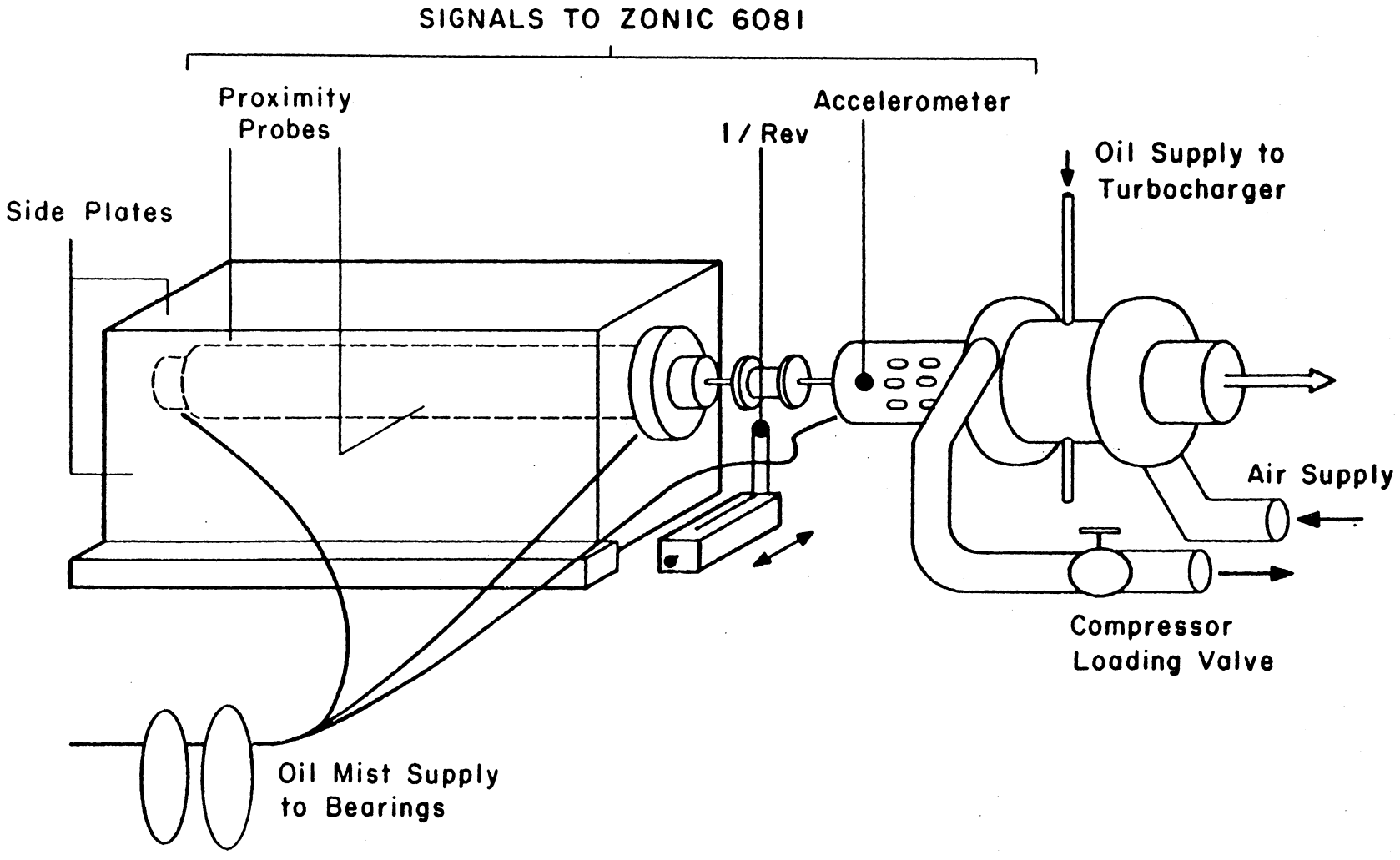

Figure 3.1 Experimental Set-Up

Table 3.1 List of Equipment

Accelerometer	--	Piezotronics Model, PCB 303A S/N 2040, Built-in amplifier
Ball Bearing for Shaft Extension	--	Barden 100H
Ball Bearings for Test Shaft	--	Barden 106H
Coupling	--	Thomas 50 cc
Dial Gage	--	Enco #699-10
FFT	--	Zonic 6080 S/N 215
Frequency Counter	--	Hewlett Packard 5326A S/N 1116A 00765
Oil Mister	--	C. A. Morgen, S/N B11-218-M1E
Oil Pump for Turbocharger w/A.C. Motor	--	Oberdorfer S/N 991R
	--	Dayton 5K601B
Power Supply for Accelerometer	--	Piezotronics 480A, S/N 3934
Power Supply for Proximeter Probes	--	Hewlett Packard 723A, S/N 5H1123 @ 22.5 V
Power Supply for Speed Pick-up	--	GSC, GDFM-5
Proximeter Probes (2)	--	Bentley Nevada 21500-00-32-10-02 S/N 423437 S/N 423436
Proximeter Probe Boxes (2)	--	Bentley Nevada 7200 Series S/N 201201 S/N 201203
Real Time Display Terminal	--	Zonic 6081, S/N 243
Slide Mounts (2)	--	Unislide Velmex, Inc., A1500
Speed Pick-up	--	Hewlett Packard, HEDS-1000, 141F

Table 3.1 List of Equipment (cont.)

Test Shaft with side- and end-plates	--	Inland Motors
Terminal/Display	--	Tektronix 4051, S/N
Turbocharger	--	Roto Master 104B35 P/N 104007, S/N 44038
Turbocharger Shield		

misalignment of the drive and the test shafts. An alignment block is pinned to the test table next to the test shaft. An oil misting system is adjusted to a pressure of 30 psig and an oil flow of 24 drops per minute. It provides oil mist to the two test-rotor bearings and to one bearing supporting the drive shaft. The supply lines are a clear vinyl tubing and aluminum tubing. The oil used is Mobil DTE Light.

The instrumentation is shown in Fig. 3.2. The signal from the speed pick-up is powered by a 5 V D.C. power supply. The signal, a square wave, is feed to the frequency counter and to the SORAN processor of the Zonic 6080. The accelerometer signal travels to an 18 V D.C. battery power supply and then to channel 3 of the Zonic 6080 (channel selection is arbitrary). The proximeter probe signals travel from individual amplifier boxes to channels 1 and 2 of the Zonic 6080. The probe power supply is of variable voltage and amperage, set at 22.5 VDC and 100 mA. Data analysis is done by the Zonic 6080 and data display and manipulation is done on the Zonic 6081. Data is printed out on the printer. The Tektronix 4051 or 4052 can be used in place of the Zonic 6081, in which case the Tektronix 4631 Hard Copy Unit must be used. This set-up gives better quality plots.

Testing Procedures

A. Alignment

An alignment block is rigidly pinned to the test table. The test and drive shafts were aligned before positioning and pinning the alignment block. This was done in the following manner. The drive shaft was checked for horizontal positioning by 1) sliding a dial gage horizon-

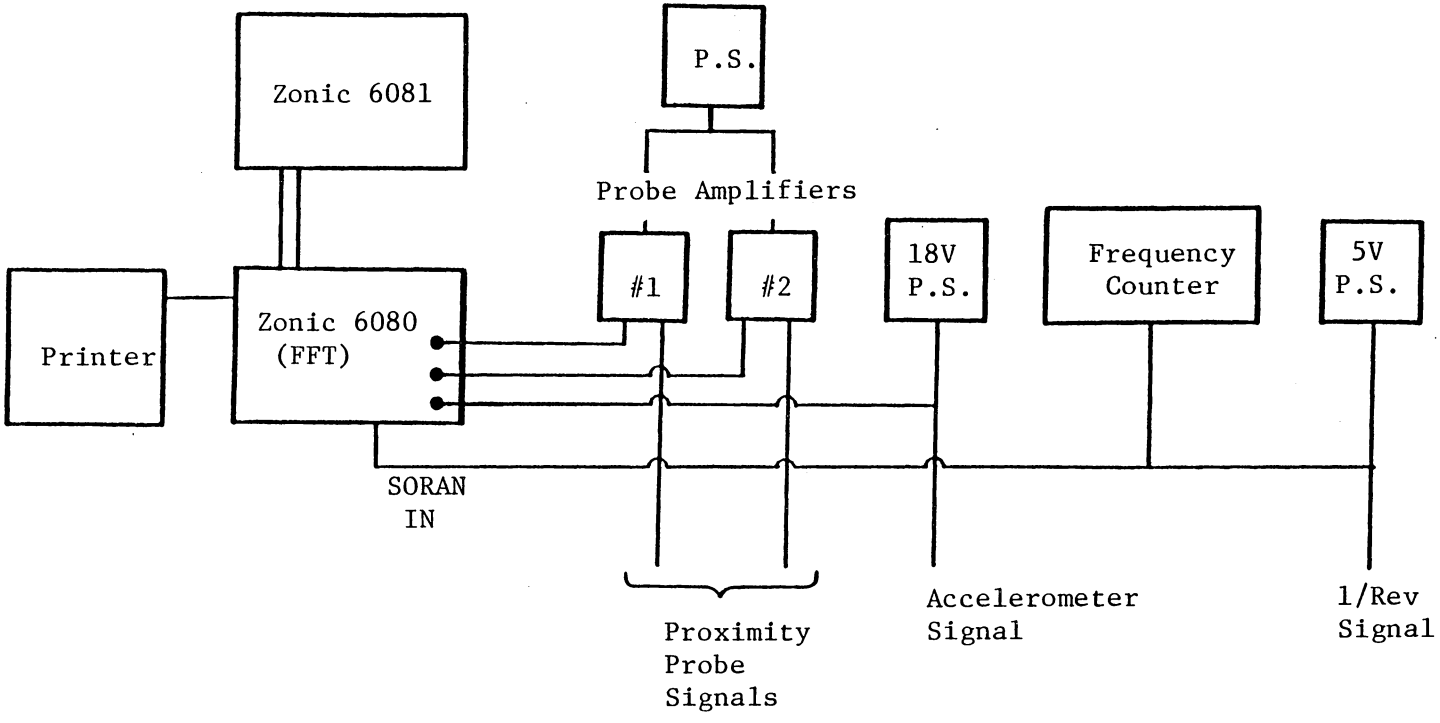

Figure 3.2 Instrumentation Diagram

tally across the top of the shaft, 2) rotating the gage positioning stand, and 3) sliding the gage across the top at another location of the shaft. The turbocharger is shimmed until the shaft is level. Next, the test shaft is aligned with the drive shaft. (Bolts mounting the base plate to the test table must be tightened before checking alignment.) Alignment is checked by 1) checking the horizontal positioning of each shaft and the relative height of one to the other, making sure the difference is equal to half the difference of the shaft diameters, 2) attaching the dial gage to either shaft, rotating that shaft, and checking the runout, making sure it is the same all the way around, and 3) sliding the gage up or down the shaft and again checking the runout. After the shafts are aligned, the alignment block is clamped to the side of the rotor base plate and pinned to the table.

With the alignment block in place, the procedures to align the system are to 1) put the coupling on one shaft, 2) slide the test shaft into place, 3) clamp the test-shaft base-plate to the alignment block, 4) tighten the bolts that mount the base-plate to the test-table, and 5) tighten the four set screws in the flexible coupling.

B. Equipment Preparation

General equipment preparation must also be done. The proximeter probes, one placed at a shaft end and one at the shaft center, should be at a distance from the shaft whose output voltage is in the center of a linear region. Probe distance is checked using the output voltage. The desired output voltage for probe #423436 is 7.5 V to 8.0 V and for probe #423437 is 7.25 to 7.75 V. Probe calibration curves are presented in

Appendix C. Probe distance should be readjusted any time disassembly is required.

The speed pick-up is adjusted to give the largest amplitude for the square wave output. The distance from the coupling producing this is approximately 0.16 inches. Final adjustment is done using a slide positioner and an oscilloscope. The distance is adjusted for maximum output voltage while the speed pick-up is focused on the black region. A set screw on the side of its slide positioner is tightened to hold this positon. This should be checked each time the test rotor is moved.

The following preparation must be done before each period of testing: 1) turn on all power supplies, 2) turn on oil pump for turbocharger oil, 3) turn on oil mister for ball bearings, 4) turn compressor loading valve about 30% of the way closed, and 5) set up the Zonic system for the desired SORAN conditions. Zonic set-up conditions are explained in the next section of this chapter.

Data Acquisition and Speed Control

The vibration data is monitored and analyzed with the SORAN option of the Zonic 6080 FFT (Fast Fourier Transform). SORAN, Sine Order Analysis, is concerned mainly with the dynamic behavior of rotating equipment. It is used to optimize spectrum analysis of periodic data and to observe how spectral components vary with running speed [1]. SORAN is used to take data at a rate proportional to shaft speed (n samples per revolution) as opposed to equal time intervals. This data collection rate is called slew rate and increases as speed increases. If the total number of data points (1024 per channel for the Zonic 6080

FFT) is evenly divisable by the number of data points per shaft revolution, then an integer number of revolutions is stored in the data block. This is desirable for a Fast Fourier Transform, as FFT analysis assumes data is period with respect to its storage block length.

Orders of the running speed are most often the frequencies of expected vibration. The Order Tracking mode of SORAN only stores vibration data at orders of the running speed and was selected as the data collection mode. The vibration signals being monitored are analyzed at selected speed increments. Each data sample is 1024 data points and takes up an entire storage block. Only one sample is analyzed at a time. No averaging is done. After analysis is completed, selected orders of the running speed are stored in memory. Other frequencies are not stored in memory. With a limited memory, this allows smaller speed increments to be used and, therefore, more data points per order can be stored. The data taking procedures are explained in the following paragraphs.

In order to take data, SORAN must first be initialized by entering "SI". The analysis type must be selected and the set-up conditions set. The analysis type Tracking Order-Spectrum is selected by entering "SOR 3,1". Figure 3.3 shows the set-up conditions used for one run. Conditions 6 and 7 are changed according to the desired speed range and number of samples. Conditions 9 and 10 can be changed after data is acquired to access the different channels and orders. The other conditions should be set as shown in Fig. 3.3.

Next, the drive unit is supplied with enough air to run at a low speed, i.e., under 2,000 rpm. This is done by adjusting the control

```
*****  Order Tracking, Fixed Order vs RPM  *****
 1.) TACHS/ REV:  . . . . . 1.000E+0
 2.) SAMPLES/ REV . . . . . 3.200E+1
 3.) MAX USABLE ORDER:  . . . . . 1.250E+1
 4.) WINDOW #:  . . . . . .1
 5.) LINES/ ORDER:  . . . . . 3.200E+1
 6.) RPM RANGE: . . . . . 1.000E+3 , 3.500E+4
 7.) MIN INCREMENT: . . . . . 5.000E+2
 8.) SPEED  (UP/DOWN 1/0):  . . . . . .1
 9.) DISPLAY ORDER #: . . . . . 1.000E+0
10.) AMPL AXIS - Log/Linear (1/0):  . .0
11.) AMPL AXIS - # Decades: . . . . . .3
12.) MAX VALUE: . . . . . 1.000E+2
13.) ORDERS TO STORE: . . . . . 1.000E+0 ,  2.000E+0
                      . . . . . 3.000E+0 ,  4.000E+0
14.) REAL TIME TABULATION (1=ON,0=OFF) : 0
15.) PF RPM RANGE:  . . . . . 1.000E+3 , 3.500E+4
16.) CH PAIR(S):  . . . . . 2/1   3/1
17.) DISPLAY CH# OR CH PAIR (INPUT#, OUTPUT#): 1
18.) DISPLAY TYPE: (CH SELECT DETERMINES CH # OR RATIO)
 (0. No display during data acquisition)
 (2. Magnitude )
 (3. Phase )
 (4. Real )
 (5. Imaginary )
 (6. Nyquist )  . . . . . .2
19.) CROSSHAIR (YES/NO 1/0):  . . . . .0
+)
```

Figure 3.3 Set-Up Conditions for the FFT

valve. This is done slowly to have better control over the speed, as there is a lag in response time. Once a slow speed is maintained, "RPM" is entered on the Zonic system and the variable resistor is adjusted until updates of the speed are displayed on the Zonic 6081. "CNTR-C" stops the RPM measurement display. The speed of the turbocharger unit is then reduced to zero rpm. "GO" is entered and the turbocharger unit is run through the speed range in the set-up conditions. The turbocharger unit should be run through natural frequencies relatively fast to avoid possible vibratory damage. The speed is then quickly reduced to zero rpm. If the high speed in the set-up conditions is not reached, "CNTL-C" must be entered in order to access the data. "DO" is entered to display order amplitude vs. speed. "PO" is entered to display the same information in tabular form. Condition 9 of the set-up conditions selects which order is displayed and condition 17 selects from which channel.

RESULTS

Only three preliminary tests were completed due to equipment failure. Each test employed one proximity probe positioned horizontally at the center of the shaft between bearings, and another probe positioned vertically just to the inside of one bearing. For the first two tests, vibration data were taken over a range of 1,000 rpm to 35,000 rpm in increments of 500 rpm or greater. For test three, data were taken over a range of 2,000 rpm to 56,000 rpm in increments of 200 rpm or greater. Natural frequencies are determined on frequency response plots (FRPs) from vibration amplitudes that are greater than background vibration levels. These increased vibration levels are henceforth referred to as peaks.

Frequency Response Plots were recorded for orders one through four for each probe position of each test. Many of these plots showed slightly increased vibration levels at expected running speeds for resonances and their harmonics, especially for orders one, two, and three. There were also vibration peaks that occurred at running speeds not corresponding to natural frequencies. This is discussed in the "Discussion and Conclusions" section. Most of the fourth order plots showed no increased vibration levels at expected frequencies.

Four plots, Figures 4.1 through 4.4, are representative of many of the better plots, showing increased vibration levels at expected running speeds. Figure 4.1 is a first order plot and should show natural frequencies. There is an increased vibration level from approximately 19,500 rpm to 23,000 rpm corresponding to the first natural frequency. A slight vibration increase corresponds to the second natural frequency

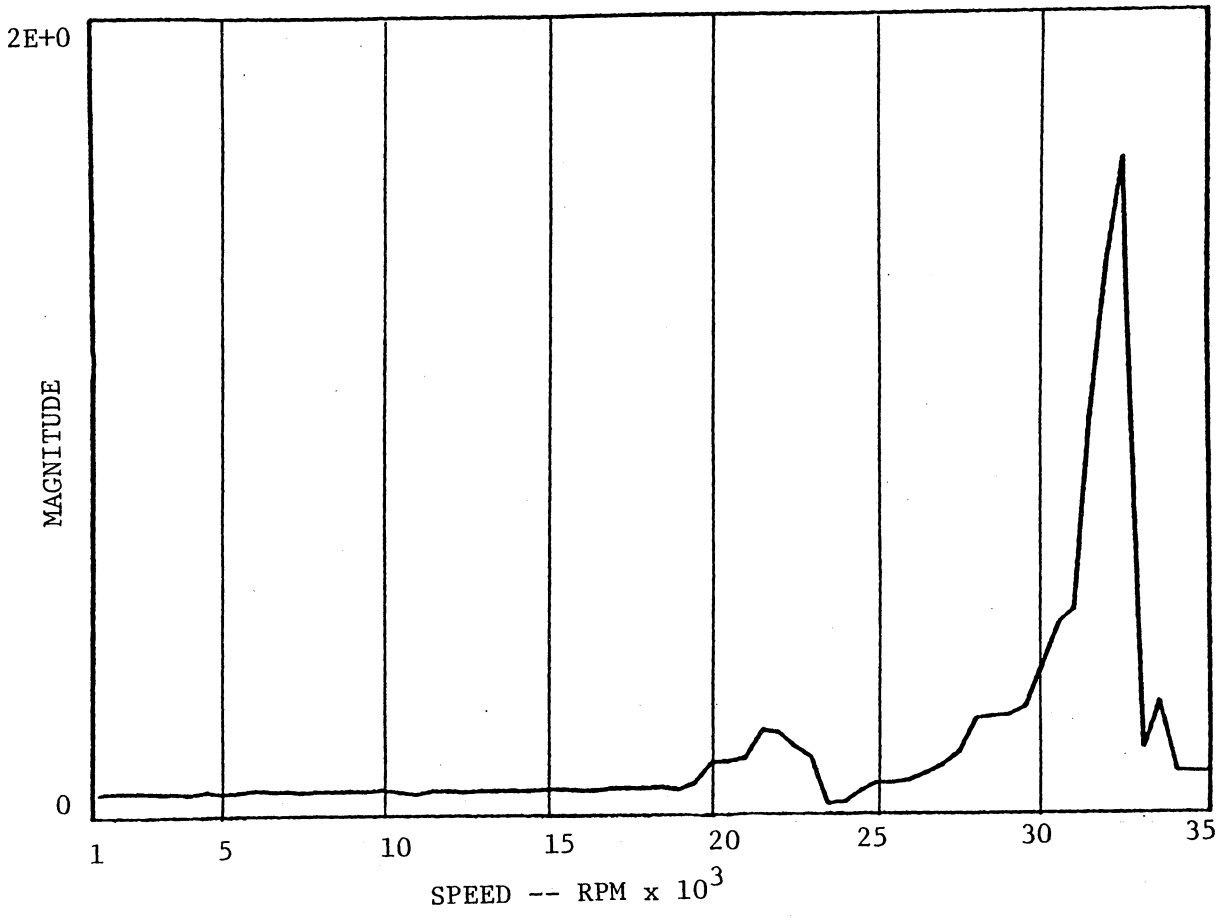

Figure 4.1 Shaft Center Frequency Response Plot, Order 1

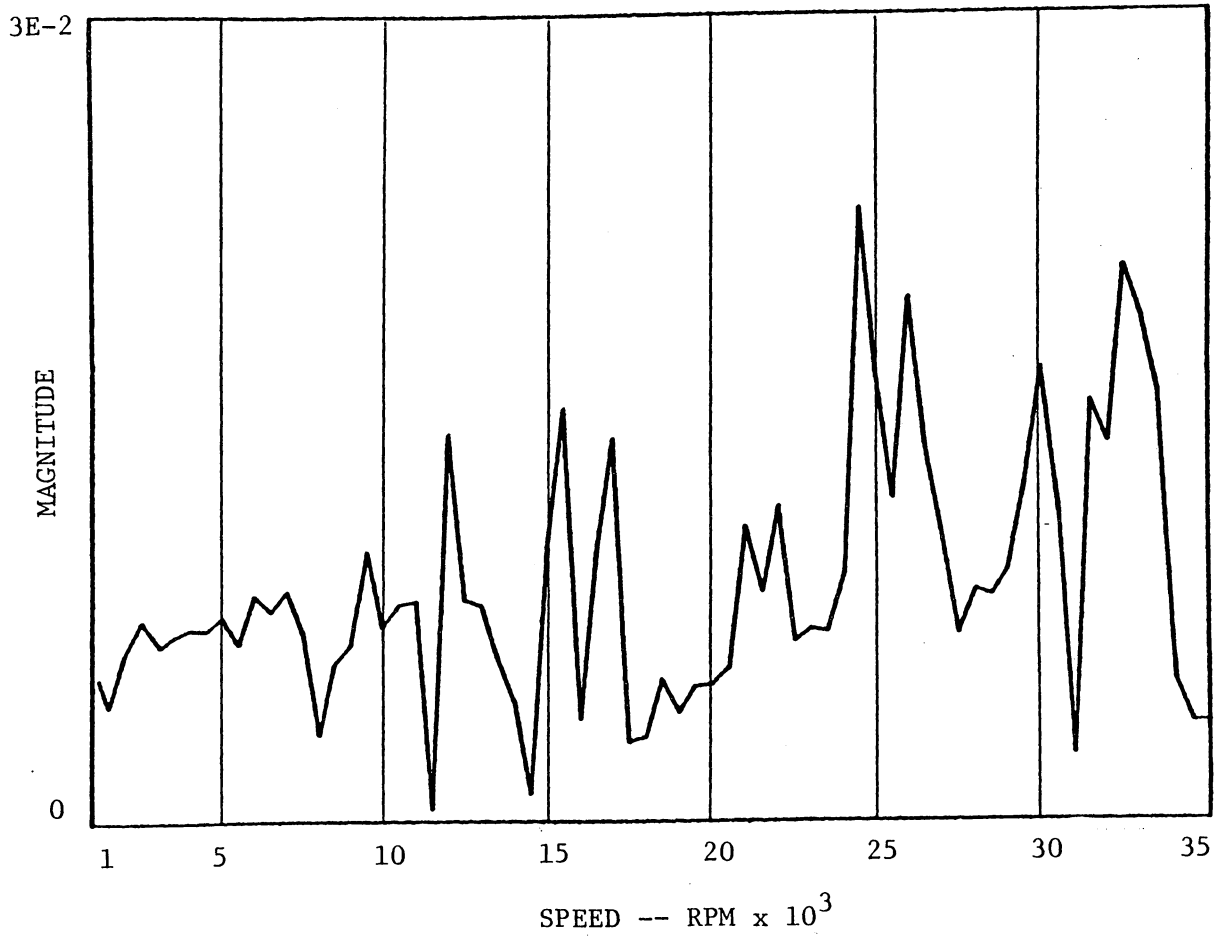

Figure 4.2 Shaft End Frequency Response Plot, Order 2

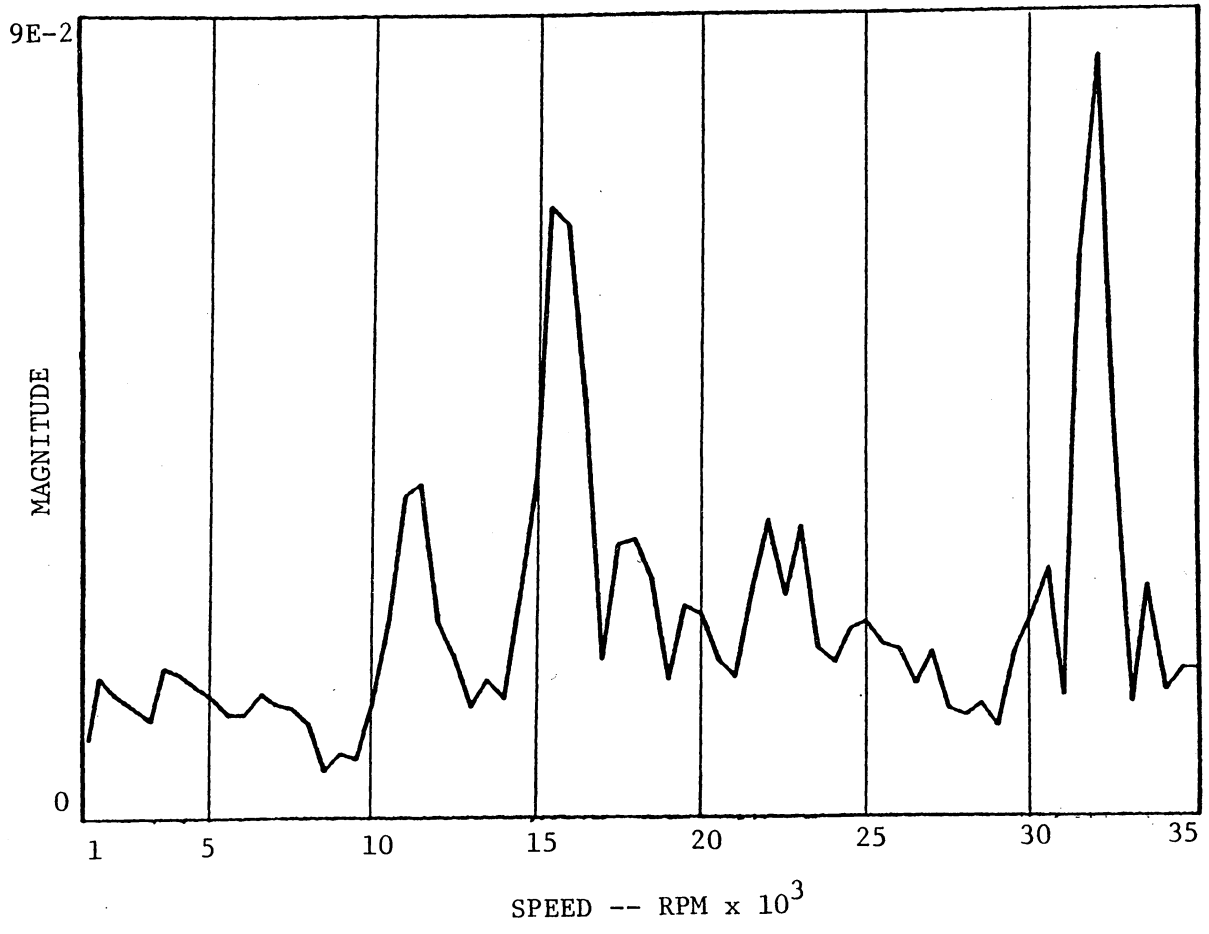

Figure 4.3 Shaft Center Frequency Response Plot, Order 2

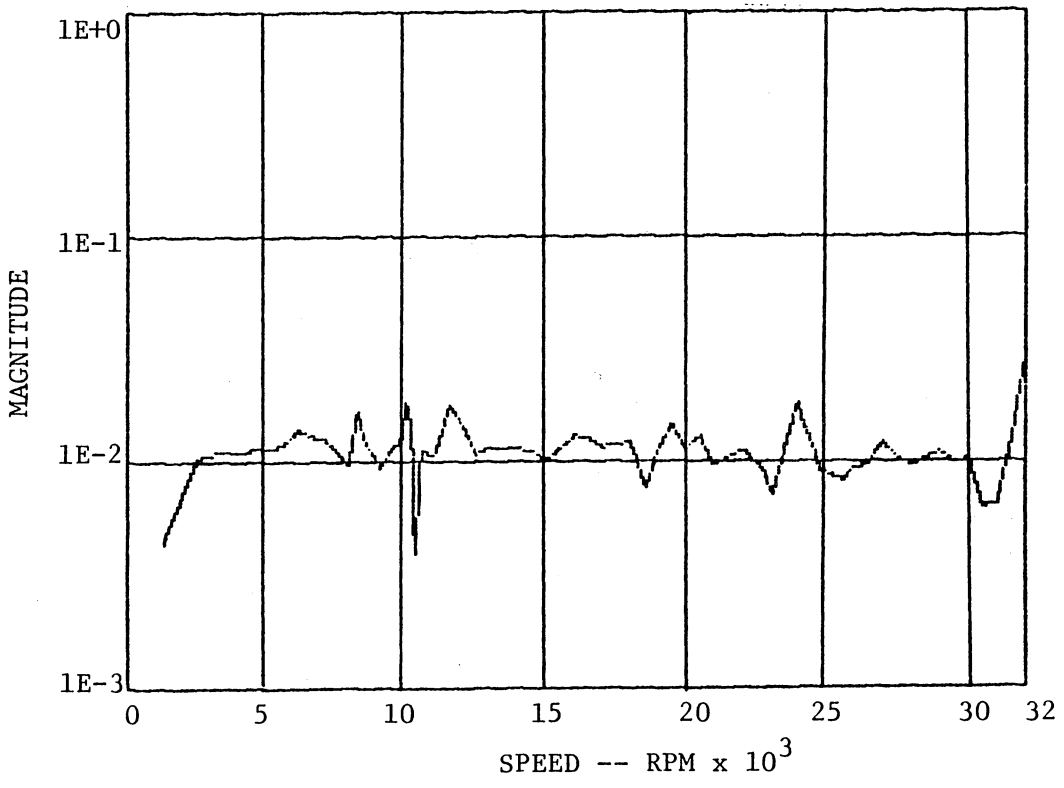

Figure 4.4 Shaft Center Frequency Response Plot #2, Order 3

at 25,400 rpm. A larger increase in vibration at around 27,500 rpm corresponds to the third natural frequency. The vibration peak around 32,000 rpm is thought to be due to the drive unit and is discussed in the "Discussion and Conclusions" section.

Figure 4.2 is a second order plot. A peak at approximately 12,000 rpm, decreasing to a background level at around 14,000 rpm, corresponds to the second harmonic of the first natural frequency. Two peaks in the range of 15,000 to 17,500 rpm correspond to the second harmonics of the second and third natural frequencies. The double-peaked swell from 21,000 to 22,500 rpm could correspond to the second harmonic of the fourth natural frequency. A peak at 24,000 rpm corresponds to the second harmonic of the fifth natural frequency.

Figures 4.3 and 4.4 also have peaks corresponding to the second and third harmonics, respectively, of the first five natural frequencies. Figure 4.5 is a Campbell diagram displaying the measured harmonic vibration peaks in comparison with the analytical analysis.

No attempt to verify mode shapes was done because not enough information was available from the data. A minimum of three probes in each direction would be necessary to confirm bending modes. The two probe locations used were 1) half-way between bearings and 2) just to the inside of one bearing, one in the x-direction and the other in the y-direction. The mode shapes determined analytically and noted in Table 2.4 are for one direction or the other.

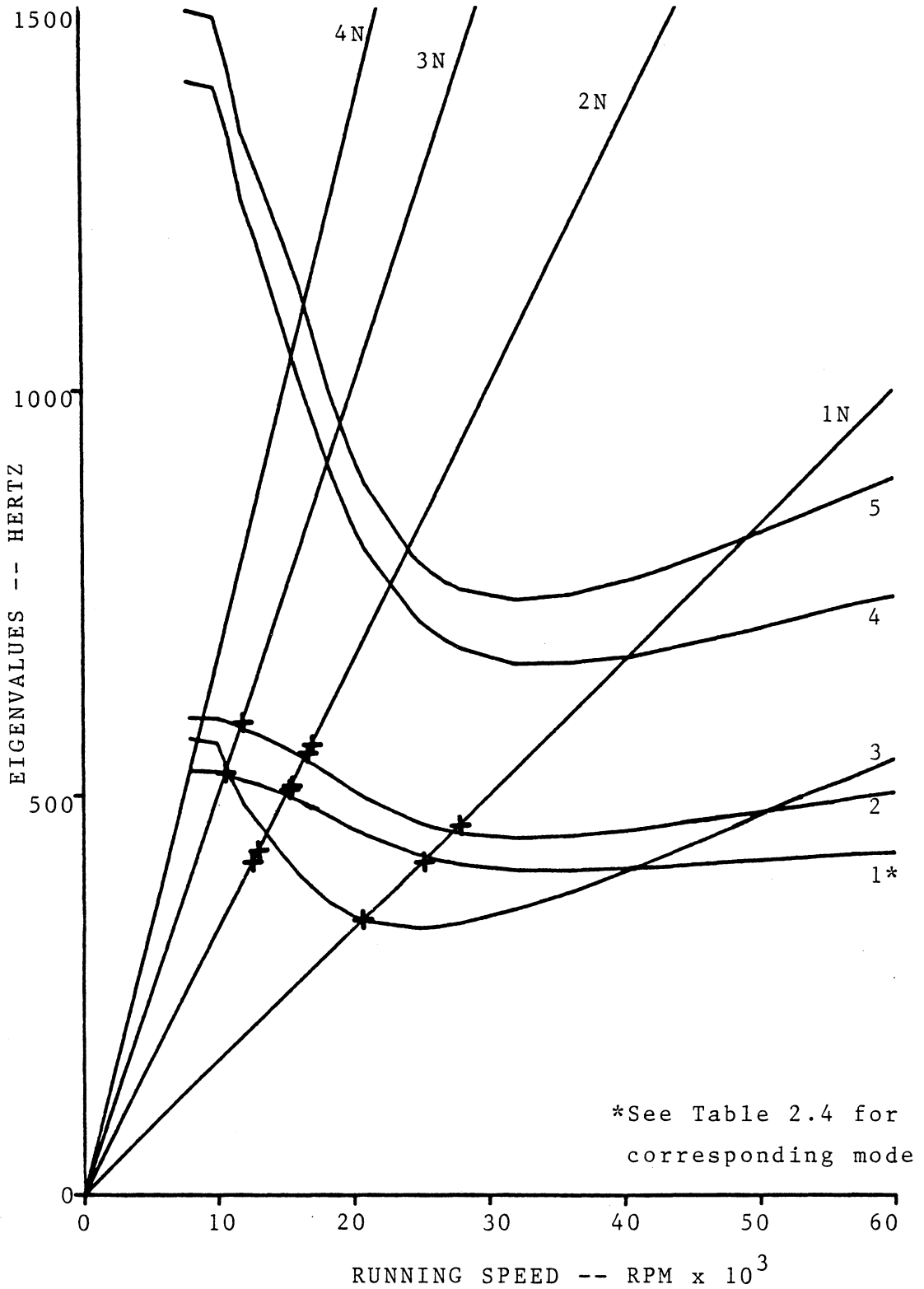

Figure 4.5 Comparison of Analytical and Experimental Results

DISCUSSION AND CONCLUSIONS

Comparison between analytical and experimental results presented in Figure 4.5 shows that the selected frequency response plots (Figures 4.1 through 4.4) show peak values which agree with expected natural frequencies and their harmonics. However, there are many vibration peaks of approximately the same amplitude that do not correspond to any critical speeds determined analytically.

Most of the peaks noted from the frequency response plots are low level (less than 0.1 volts). With a sensitivity of 0.45 Volts/mil for the proximity probes, these peaks represent less than 1/2 mil of vibration. It seems likely that the misalignment of less than one mil did not cause large enough forces and moments to excite natural frequencies to noticeably high vibration levels. In this case, some of the low level vibrational peaks would represent low level excitation of critical speeds. It is also possible that many of these peaks are near background vibrational levels and show up because the method used for taking data did not use data averaging. Amplitude variations in vibration levels occur from one revolution to another and, without averaging data points, these variations show up as slight decreases or increases in vibration. Although the Order Tracking mode of SORAN does not actually average data, it can accomplish effectively the same thing by obtaining data for n revolutions (32 revolutions for the tests completed) in one data sample. Then the spectral analysis is for n revolutions instead of 1 revolution. The slew rate must be slow enough

for each of the n revolutions to have effectively the same running speed. However, there is no way to tell if the tests completed were run slowly enough. This is discussed further in the "Recommendations" section.

There are also some high vibrational amplitude peaks not corresponding to analytically determined critical speeds. Several of these occur in the range of 30,000 to 35,000 rpm on the first-order harmonic frequency response plots. This speed range is not near any of the expected shaft critical speeds. However, it is in the same frequency range as that of the high vibration levels of the air-driven high-speed drive. This implies that these high vibration levels are transmitted from the drive system to the shaft, and that the shaft and bearing system and the high-speed drive are not absolutely isolated from each other. They, along with the coupling, compose a system different from the one that was modelled analytically. This changes system parameters such as mass and stiffnesses which can change natural frequencies.

Because no averaging was done while taking data, normal variation in vibration amplitudes may show up as small peaks. Averaging would smooth the curves of the frequency response plots, allowing speeds with a constant increase in vibration levels to be noted. On this basis, and in an attempt to clarify the data, the frequency response plots were analyzed by ignoring small vibration peaks that could be due to normal data variation and by following the general curve. Analytical modes shapes and relative vibration amplitudes were also compared. However, this analysis added no clarification to the previous analysis.

Although most of the critical speeds and harmonics have corresponding vibration peaks, it is very likely that the misalignment between the drive and the shaft was not enough to excite critical speeds to measurable levels. Many of the vibrational peaks noted may be due to no averaging in the data taking process; however, some of these may represent critical speeds. Also, the drive system and the shaft are not perfectly isolated and possibly should have been modelled, with the coupling, as the complete test system. Noting these possibilities, the results of this investigation must be considered inconclusive as an evaluation of the low-speed harmonic excitation technique for predicting critical speeds.

RECOMMENDATIONS

Although the results from these tests are inconclusive, they do indicate that low-speed harmonic excitation of high-speed natural frequencies using a misaligned disc coupling may be a useful tool for predicting resonances without actually running through the higher speeds. Recommendations that may aid in obtaining more conclusive results are discussed.

A model of each component of the entire test system, separately and then together as a whole system, would give more realistic analytical results. Unless components are well isolated from each other 1) the resonances due to one component may be seen in another, 2) the resonances in individual components may shift, and 3) system resonances, separate from resonances of components, may develop. In the tests done, high vibrations due to a resonance of the drive unit were transmitted to the test shaft. For this particular test set-up the individual components to be modelled would be the drive unit, the disc coupling, and the shaft- and-bearing unit.

Greater shaft misalignments should be employed. Since misalignment less than 0.001" was apparently not enough to generate sufficient forces to excite natural frequencies, a misalignment of 0.003" to 0.005" is recommended. The misalignment could be increased more if necessary, but small increments should be employed in order to avoid catastrophic damage.

In conducting tests on the shaft-and-bearing system, control of the running speed was poor. The acceleration of the high-speed air-drive turbocharger drive unit varied with running speed. In addition there

was a lag effect using the hand operated flow control valve. This is not desirable and affects the data collected in the Order Tracking mode of SORAN. As acceleration changes, slew rate (corresponding to data collection rate) changes. The slew rate is the change in RPM divided by the total time to acquire data, spanning 1024 data points. If the slew rate is too high, then 1) the minimum (speed) increment will be exceeded, and 2) the running speed at which data is taken may exceed the speed which SORAN has determined to be the running speed for that data sample. The actual and the determined running speeds of a data sample may then be separated by more than the frequency resolution and would then be represented by separate spectral lines. For Order Tracking, only requested orders are stored, and the spectral line for the running speed determined by SORAN is stored. For order one, the difference in amplitude between the actual and determined running speeds should not be great. However, for the n^{th} orders, the frequency difference for the actual and determined running speeds is n times as great as for order one, and the change in amplitude of corresponding spectral lines may be significant. Only the spectral line corresponding to the running speed determined by SORAN is stored. If this were the case, a harmonic of a natural frequency having an increased vibration level might not show up as such. It is not possible to tell if the tests completed were run too fast.

It is possible to see if the slew rate is too fast by using SOR (1,1), the Order Spectrum mode. However, this must be done on a separate test run and there would be no guarantee that the slew rate would be the same on a data collecting test run.

There are four possibilities for taking care of the slew rate problem. One is to use the Maximum Flat Top window. This data window has a larger frequency resolution. This is worse for determining the running frequency, but because the resolution is 2.3 times larger, a spectral line has that much more chance of including both the actual running speed and the running speed determined by SORAN. The spectral line amplitude is that of the frequency (in the spectral-lines frequency range) with the highest vibration level. Although this method is likely to solve the problem of a high and varying slew rate, it cannot be guaranteed to do so. The second option of solving the problem is to run through the speed range very slowly. However, it may be difficult to control the acceleration well enough to eliminate the possibility of running at a natural frequency for an inadvisable length of time.

The third option is to use either the Spectral Cascade mode or the Order Cascade mode of SORAN. In this case, the entire frequency spectrum for each sampling speed is displayed on the CRT, not just the orders. Vibration peaks and their frequencies can be determined from this plot even if the running speed is different from what SORAN has determined to be the data-collecting running speed. The slew rate would still need to be slow; however, it can be better controlled by watching the plot being generated as the test is being conducted. Also, for two (or three) probes, twice (or three) times as many tests would have to be run because only one channel is displayed. After the screen is cleared another cascade cannot be generated without another test.

The fourth option is to use an automatic control valve with a feedback from the speed indicator to control the air flow to the turbocharger, and thereby control the speed more closely.

Another recommendation is to take data at smaller speed increments. If this were done, the slew rate would have to be even more carefully controlled; however, for order plots, vibration information would be available for more speeds.

The last recommendation is to consider different types of driving units. The turbocharger modified into a drive unit by itself had very high vibration levels that contributed to equipment failures. It also seemed sensitive to the forces applied by the coupling and test shaft. These problems might be due largely to the shaft extension and housing; however, this is not definite.

REFERENCES

1. Zonic Corporation, "SORAN", 6080 System Manual, Milford, Ohio, 1980.

2. Hampton, Jeffrey Jon An Investigation of the Three-Dimensional Vibration Characteristics of a Rotor-Bearing System Using the Finite Element Method, Thesis, Virginia Polytechnic Institute and State University, February 1982.

3. Van Winkle, Steven T., Predicting the Dynamic Behavior of Rotor Systems on Ball Bearings, Thesis, Virginia Polytechnic Institute and State University, October 1980.

4. Hampton, J. J., "Comparison of T. A. Harris, Van Winkle, and Air Force Bearing Analysis Methods," [Memo, Virginia Polytechnic Institute and State University, February 1981].

5. Jones, A. B., et. al., Rotor-Bearing Dynamics Technology Design Guide, Part II: Ball Bearings, Shaker Research Corporation, Ballston Lake, New York, February 1978.

6. Stargardter, H., "Dynamic Models of Vibrating Rotor Stages," ASME Paper 66WA/GT-8, New York, NY, November 1966.

7. Trumpler, Jr., W. E., and Owens, H. M., "Turbine-Blade Vibration and Strength," Transactions of the ASME, April 1955.

8. Owens, H. M., and Trumpler, Jr., W. E., "Mechanical Design and Testing of Long Steam Turbine Blading," ASME Paper 49-A-64, New York, NY, November 1949.

9. Fleeting, R., and Coats, R., "Blade Failures in the H.P. Turbines of R.M.S. 'Queen Elizabeth 2' and Their Rectification," Institute of Marine Engineers Paper 165591, London, England, October 1969.

10. Wright, John, "Which Flexible Coupling?", Reprinted from 71/72 Power Transmission & Bearing Handbook, Koppers Company Inc., Form 7321, Baltimore, Maryland, 1972.

11. Dewell, David L., Detection of a Misaligned Metallic Disc Flexible Coupling, Thesis, Virginia Polytechnic Institute and State University, March 1980.

12. Dewell, D. L., and Mitchell, L. D., "Detection of a Misaligned Disc Coupling Using Spectrum Analysis," MSA-Mechanical Signature Analysis, pp. 19-28, ASME, New York, NY, September 1983.

13. Whetstone, W. D., EISI/SPAR Reference Manual, 4 Vol., December 1978.

APPENDIX A: High-Speed Drive

APPENDIX A

High-Speed Drive

A Rotomaster 704B35 V-2 trim turbocharger was modified to be an air-driven high-speed drive. A 7-1/8" long shaft with internal threads at one end screwed onto the compressor-end of the turbocharger shaft, and was bonded in place with a high-strength glue. A cylindrical housing was mounted over the mouth of the compressor housing and extends to support the 7-1/8" shaft extension with a bearing in its end. The 2 inches of the shaft extension extending beyond its housing was used to couple to the driven shaft. Holes in the cylindrical housing allow air to run through the compressor. A valve attached to the compressor outlet-hose was used to load the compressor. Figure A-1 shows the automotive turbocharger adapted to an air-driven high-speed drive. Figure 3.1 shows the high-speed drive in the test set-up.

From vibration tests of this high-speed drive, relatively high vibration levels were detected in the range of 30,000 to 35,000 rpm and 70,000 rpm and above. The accelerometer used to monitor vibration levels was positioned radially at the cantilevered end of the shaft-extension housing.

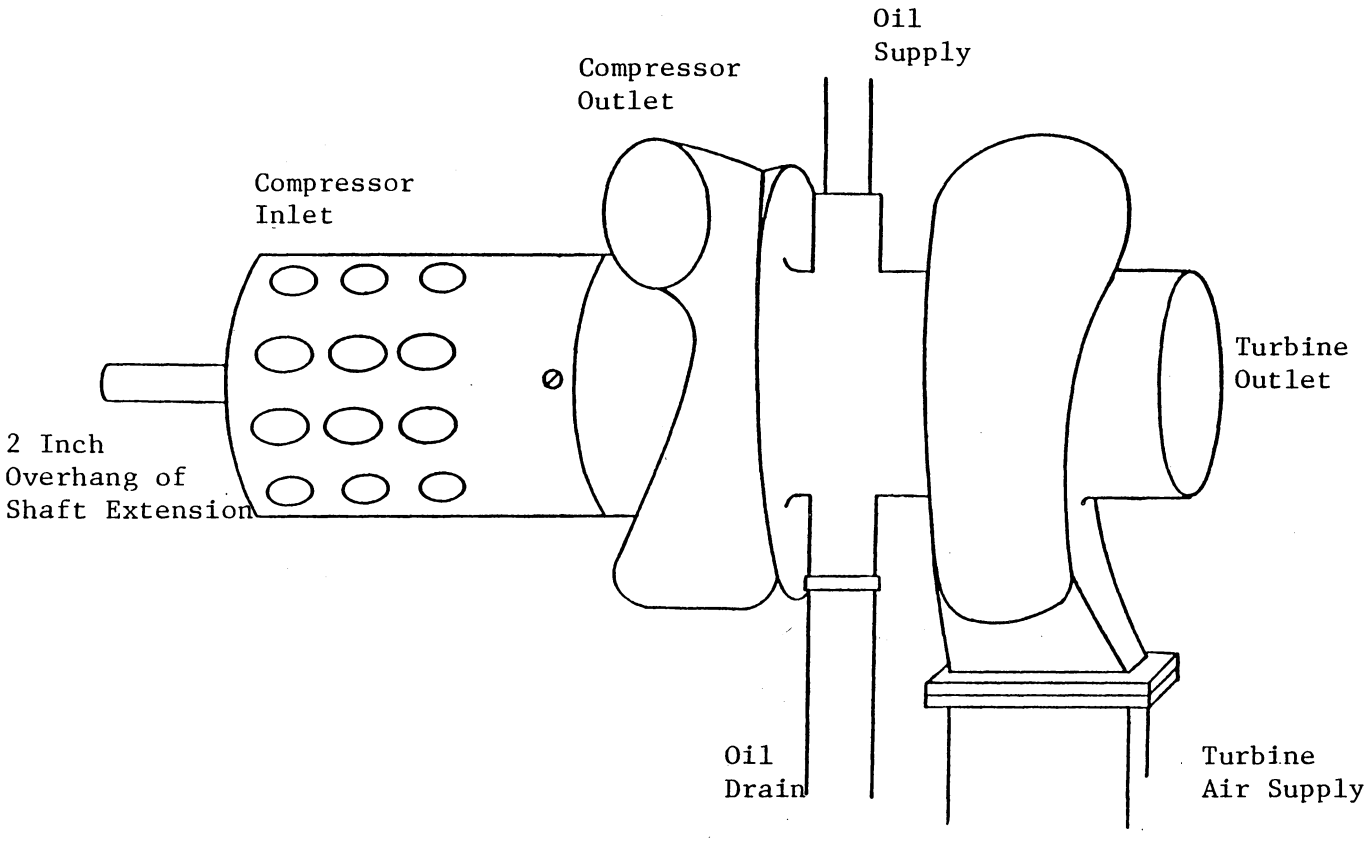

Figure A-1 Air-Driven High-Speed Drive

APPENDIX B: Spar Routines

APPENDIX B

SPAR Subroutines

The subroutines used are presented in the order in which they are submitted with a brief explanation of each. The necessary input files follow. The ElSl/SPAR Reference Manual [13] is available for further information.

TAB--creates data sets such as joint locations, material constants, section properties, and beam orientation.

ELD--forms data sets of element definitions.

TOPO--creates data sets used by subroutines K, M, and INV in the assembly of the stiffness and mass matrices and in factoring matrices.

EE--forms a file containing element information such as intrinsic stiffness, orientation, material constants, etc, used by subroutines EKS and K.

EKS--computes intrinsic stiffness and stress matrices and puts them into the element information file.

K--assembles elastic stiffness matrices in SPAR format used in subroutine INV.

INV--factors assembled system matrices.

M--assembles mass matrices.

EIG--solves linear vibration eigenproblems.

VPRT--used to display and edit information such as vibrational eigenvectors.

INPUT FILES FOR 1.5" DIAMETER STEEL SHAFT, FINAL ANALYSIS

```
TAB      INPUT
START 29,6
TEXT
 CIRCULAR SHAFT EIGENVALUES--STIFFNESS FOR 20650 RPM---STEEL, 1.500"D'
JOINT LOCATIONS
1        0.0        0.0        0.0
2        0.0        0.0        1.00
3        0.0        0.0        2.50
4        0.0        0.0        2.75
5        0.0        0.0        4.0
6        0.0        0.0        4.75
7        0.0        0.0        5.5
8        0.0        0.0        6.25
9        0.0        0.0        7.0
10       0.0        0.0        7.75
11       0.0        0.0        8.5
12       0.0        0.0        9.25
13       0.0        0.0        10.0
14       0.0        0.0        10.75
15       0.0        0.0        11.5
16       0.0        0.0        12.25
17       0.0        0.0        13.0
18       0.0        0.0        13.75
19       0.0        0.0        14.5
20       0.0        0.0        15.25
21       0.0        0.0        16.0
22       0.0        0.0        16.75
23       0.0        0.0        17.5
24       0.0        0.0        18.25
25       0.0        0.0        18.50
26       0.0        0.0        20.00
27       0.0        0.0        21.00
28       0.0        0.0        3.875
29       0.0        0.0        17.75
MATERIAL CONSTANTS
1  30.+6  0.289  0.283  0.65-5
BEAM ORIENTATION
  1  1  1  1  1.
E21 SECTION PROPERTIES
GIVN 1   0.04909     0.  0.04909     0.  0.78540  0.098175   0.  0.  0.
GIVN 2   0.09517     0.  0.09517     0.  1.0936   0.1903     0.  0.  0.
GIVN 3   0.24850     0.  0.24850     0.  1.76715  0.49701    0.  0.  0.
GIVN 4   0.0009707   0.  0.0009707   0.  0.11045  0.0019414  0.  0.  0.
BEAM S6X6
1  1.8670+5
     0.          1.8453+5
    9.5363+3      0.         5.1583+4
     0.         -5.0553+4     0.         1.9196+4
   -5.1041+4      0.        -2.4927+3     0.         1.9317+4
     0.           0.          0.          0.          0.          1.
CON 1
ZERO  1  2  3  4  5:28:29
```

```
ELD       INPUT

E21
NSECT=1
NMAT=1
2  3:25  26:26  27
NSECT=2
NMAT-1
3  4:4  5:23  24:24  25
NSECT=3
5  6:6  7:7  8:8  9:9  10:10  11:11  12:12  13:13  14:14  15:15  16:16
17:17  18:18  19:19  20:20  21:21  22:22  23
NSECT=4
1  2
E22
NSECT=1
28  4:29  24

M         EXEC

&CONTROL OFF
GLOBAL TXTLIB FOR TXLIB VPIUTIL CMSLIB
FI 06 DISK M OUTPUT D
FI 30 TERM
FI 31 DISK FT31 M D(RECFM VBA LRECL 133 BLOCK 137
FI 40 DISK FT40 M D(RECFM VBA LRECL 133 BLOCK 137
LOAD DUMLIB DRIV M SPARLIB PRWFIL SEARCH(CLEAR
START

M         INPUT

RESET IBEAM=0
RESET G=386.

EIG       INPUT

RESET M=CEM,INIT=9,NREQ=8
```

APPENDIX C: Proximeter Probe Calibration Curves

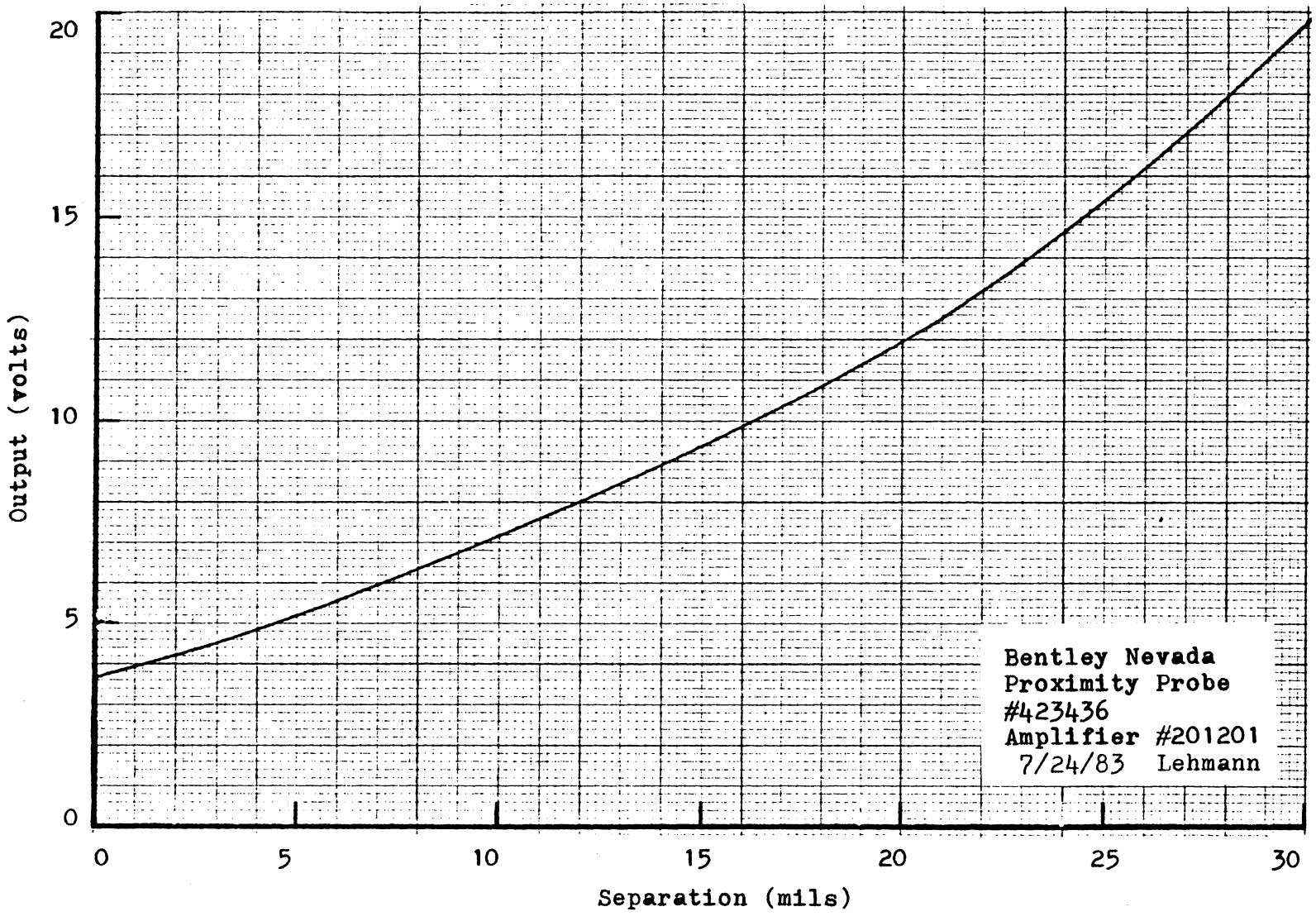

Figure C-1 Calibration Curve for Proximity Probe #423436

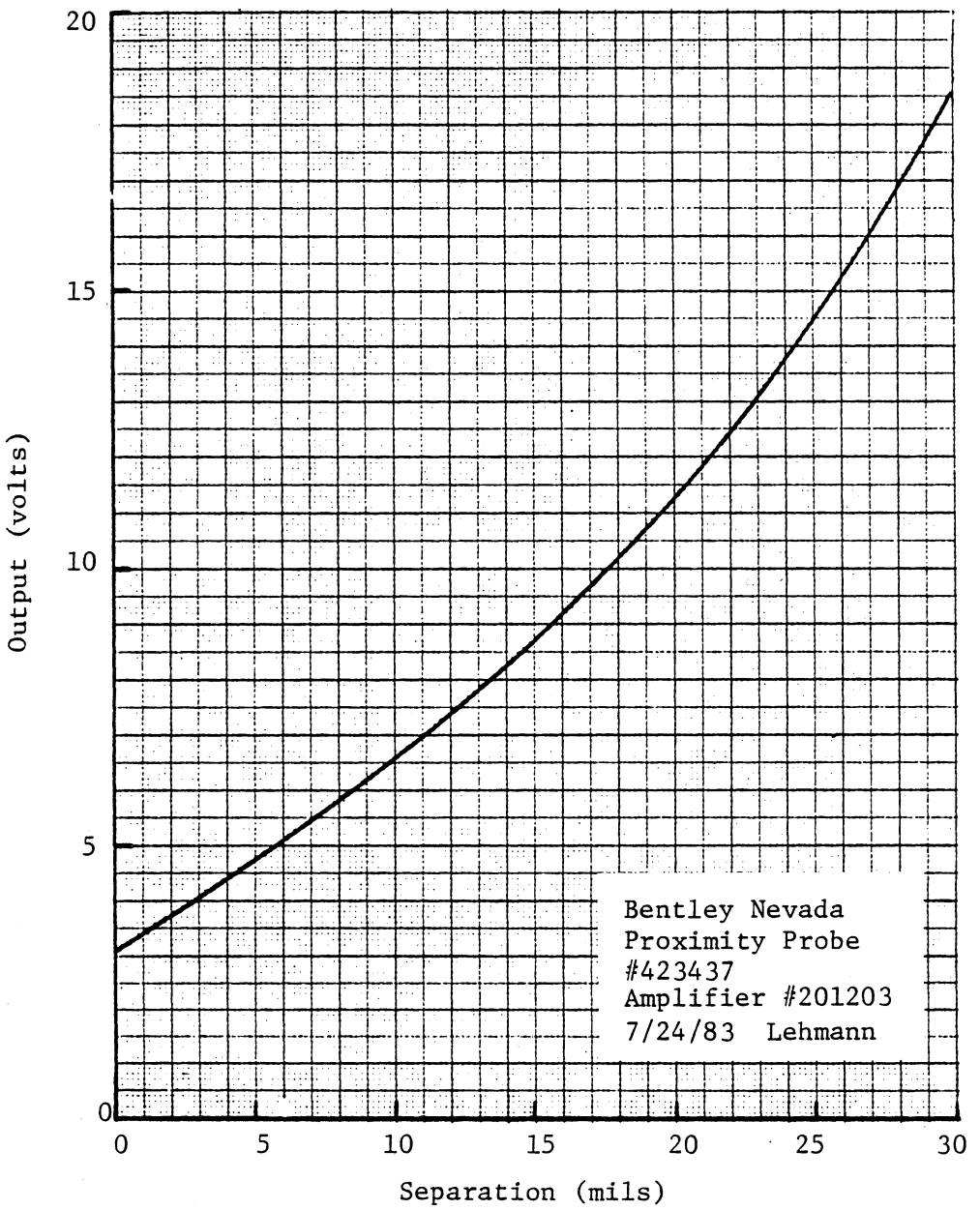

Figure C-2 Calibration Curve for Proximity Probe #423437

The vita has been removed from the scanned document